New results on the Stark and Zeeman effects in the hydrogen atom

V. S. Lisitsa

I. V. Kurchatov Institute of Atomic Energy, Moscow

Usp. Fiz. Nauk **153**, 379–421 (November 1987)

The review deals with a new range of problems related to the Stark and Zeeman effects in the hydrogen atom, which have attracted a growing interest in these effects during the last decade. These problems include the behavior of a highly excited hydrogen atom in fairly strong electric (F) and magnetic (B) fields. All the parameters describing the behavior of an atom in the fields F and B are considered: changes in the energy levels, lifetimes of the states, intensities (oscillator strengths), decay probabilities, nature of atomic electron trajectories, including the possibility of their stochastization. Both analytic and numerical solution methods are described. Much attention is given to semiclassical and purely classical approaches, which are being developed rapidly. The review is designed to provide a description of the methods without the need to refer to the literature.

CONTENTS

1. INTRODUCTION

Investigations of the splitting of the energy levels of atoms in an electric field F (Stark effect, 1913) and in a magnetic field B (Zeeman effect, 1896) have provided one of the important confirmations of the validity of the main assumptions of quantum theory. Fundamentals of the quantum theory of the Stark and Zeeman effects are treated in detail in the well-known monograph of Bethe and Salpeter,[1] and also in textbooks on quantum mechanics[2] and theoretical spectroscopy.[3]

In recent years the interest in these effects has shifted to applications. It has been found that many theoretical results are not very suitable for specific calculations or are still incomplete. Further development of the theory has involved mainly investigations of atomic spectra in strong fields B and F and of highly excited states characterized by $n \gg 1$. The interest in these problems arises because of a wide range of applications such as ionization in an electric field of Rydberg atomic states populated selectively by laser radiation,[4,5] absorption spectra of excitons in a magnetic field,[6,7] structure of atoms in very strong magnetic fields on the surfaces of neutron stars,[8–10] splitting and broadening of atomic spectral lines by electric and magnetic fields in a plasma,[3,11,12] structure of rf lines emitted by highly excited atoms in the interstellar medium,[13,14] etc.

Recent experiments on Rydberg atoms have been carried out in connection with a wide range of theoretical problems including the quantum defect method,[15] the dynamic Stark and Zeeman effects in alternating fields F and B (Ref. 16), and other topics (discussed in a monograph of Stebbings and Dunning[17]). An important place among these problems is occupied by the simplest atomic system, which is the hydrogen atom to which the present review is devoted.

Selective population of hydrogen states with $n \sim 10$–50 has been detected under laboratory conditions (for a review see chapter by P.M. Koch in Ref. 17, p. 473). These experiments provide, in principle, a technique for precision measurements of fundamental atomic constants. The hydrogen atom is also of great interest in astrophysics because it can be excited to states with $n \sim 100$–400 in space (for a review see chapter by A. Dalgarno in Ref. 17, p. 1). In the interpretation of both laboratory and astrophysical data one requires detailed information on the dependences of atomic parameters on the intensities of external fields and on the individual quantum numbers of atomic states. Therefore, the account given below is designed not only to introduce the general theoretical principles, but also to provide specific analytic and numerical results suitable for use in many applications. At the same time an attempt will be made not to omit problems of fundamental nature. They include, above

 0038-5670/87/110927-25$01.80

all, the existence of an additional integral of motion of an electron moving in Coulomb and magnetic fields, and the possibility of stochastization of the electron motion in this case. These problems are related closely to the fundamental principle of quantization of systems with inseparable variables.

It is surprising that in spite of the traditional nature of the topics related to the Stark and Zeeman effects, a whole series of new results have been obtained and many new observations have been made. This has revealed major capabilities of the semiclassical and purely classical solution methods. The success of the classical approach is clearly due to the incompleteness of the classical descriptions of the atom which have been "prematurely" elbowed out by establishment of the theoretical apparatus of quantum theory. Quantum-mechanical calculations based on perturbation theory, asymptotic approach, and numerical solutions of the Schrödinger equation are treated fully in the monograph of Stebbings and Dunning.[17] Therefore, we shall concentrate our attention on semiclassical methods.

We shall frequently use the atomic system of units (a.u.) without mentioning the fact explicitly. However, in some cases it is convenient to retain dimensional units. We shall therefore mention straight away the characteristic ranges of the fields F and B. The intraatomic electric field F_A is

$$F_A = ea_0^{-2} \approx 5.1 \cdot 10^{11} \text{ V/m}, \tag{1.1}$$

where e and m are the charge and mass of an electron, and $a_0 = \hbar^2/me^2$ is the Bohr radius.

In the case of magnetic fields it is convenient to introduce a field B_0 such that the magnetic interaction $\mu_B B_0$ ($\mu_B = e\hbar/2mc$ is the Bohr magneton) is comparable with the scale of the atomic energy $\text{Ry} = me^4/2\hbar^2$:

$$B_0 = \frac{\text{Ry}}{\mu_B} = 2.35 \cdot 10^5 \text{ T}. \tag{1.2}$$

The magnetic field B_A inside an atom is in fact less by a factor $(\hbar c/e^2) \approx 137$ because of the nonrelativistic nature of the motion of electrons:

$$B_A \approx \frac{B_0}{137} \approx 1.7 \cdot 10^3 \text{ T}. \tag{1.3}$$

The values (1.1)–(1.3) of the fields F_A and B_0 are very high and they are attainable only under fairly exotic conditions. However, we must bear in mind that these fields decrease rapidly on increase in the principal quantum number n of the atom. For example, the critical electric field F_c which suppresses the potential barrier of an atomic electron is

$$F_c = \frac{F_A}{16n^4}, \tag{1.4}$$

which is five orders of less than the atomic field F_A if $n \approx 10$.

Similarly, hydrogenic excitations in a solid (excitons) correspond to effective values $B_0 \sim 10$–10^2 T because of a reduction in the effective mass of an electron in a solid and also because of the high permittivity. Therefore, many of the effects considered below occur in near-critical fields F and B, but can be observed in practice.

2. STARK EFFECT

2.1. Hydrogenic atoms in an electric field. General relationships

2.1.1. The fundamentals of the theory of a hydrogenic atomic in an electric field F are well known and have been presented in detail in, for example, the monographs mentioned earlier.[1-3] However, from the point of view of practical applications many topics of this theory have not been finally resolved until very recently. This applies particularly to the interpretation of the spectra of highly excited atoms when the high degree of degeneracy of the hydrogen levels complicates enormously the calculations based on the direct application of the general formulas for the intensities of transitions, etc. We shall present a number of new theoretical results on the spectra of the hydrogen atom in an electric field and these provide simple and reliable analytic results suitable for the application to cases of practical interest.

2.1.2. A fundamental feature of the theory of the Stark effect is the ability to separate the variables in the Schrödinger equation for the hydrogen atom expressed in parabolic coordinates ξ and η (Ref. 2):

$$\frac{d^2\chi_1}{d\xi^2} + \frac{1}{4}\left(2E + \frac{4\beta_1}{\xi} - \frac{m^2-1}{4\xi} - F\xi\right)\chi_1 = 0, \tag{2.1}$$

$$\frac{d^2\chi_2}{d\eta^2} + \frac{1}{4}\left(2E + \frac{4\beta_2}{\eta} - \frac{m^2-1}{\eta^2} + F\eta\right)\chi_2 = 0; \tag{2.2}$$

here, $\chi_1(\xi) = f_1/\xi^{1/2}$ and $\chi_2(\eta) = f_2/\eta^{1/2}$ are the reduced wave functions (see Ref. 2); E is the energy; β_1 and β_2 are the constants of the process of separation of the variables $\beta_1 + \beta_2 = 1$; m is the magnetic quantum number.

Equations (2.1)–(2.2) are one-dimensional and they are characterized by the effective potentials

$$V_\xi = \frac{m^2-1}{8\xi^2} - \frac{\beta_1}{\xi} + F\xi, \quad V_\eta = \frac{m_2-1}{8\eta^2} - \frac{\beta_2}{\eta} - F\eta, \tag{2.3}$$

governed at short distances by the Coulomb and centrifugal terms, and at large distances by the term containing the field F (Fig. 1). We can see from Fig. 1 that the potential barrier expressed in terms of the variable η has a finite penetrability, so that an atomic electron can escape to the continuous spectrum (i.e., an atom can decay).

It is convenient to rewrite Eqs. (2.1)–(2.2) in terms of dimensionless variables $x = \nu^{-1}\xi$ and $y = \nu^{-1}\eta$, where ν is

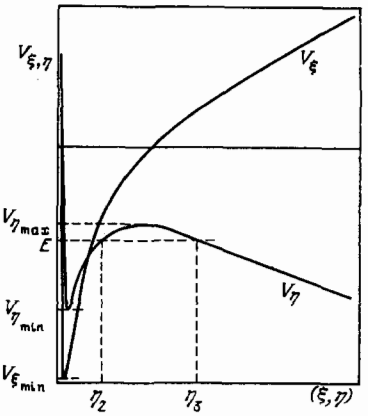

FIG. 1. Potentials $V_\xi = V_1(\xi)$ and $V_\eta = V_2(\eta)$ for the motion of an electron of energy E in an electric field, plotted using parabolic coordinates ξ and η.

the effective principal quantum number of the level, which allows for the shift of the level in an electric field **F**:

$$\nu = (-2E)^{1/2}. \tag{2.4}$$

Introducing next the reduced field intensity $w = W\nu^3$ and the new separation constants α_1 and α_2 ($\alpha_1 + \alpha_2 = \nu$) we obtain the following equations for the reduced wave functions φ_1 and φ_2 (Ref. 18):

$$\frac{d^2\varphi_1}{dx^2} + \frac{1}{4}\left(-1 + \frac{4\alpha_1}{x} - \frac{m^2-1}{x^2} - wx\right)\varphi_1 = 0, \tag{2.5}$$

$$\frac{d^2\varphi_2}{dy^2} + \frac{1}{4}\left(-1 + \frac{4\alpha_2}{y} - \frac{m^2-1}{y^2} + wy\right)\varphi_2 = 0. \tag{2.6}$$

The states of the hydrogen atom in the field F are described, as is well known,[1-3] by parabolic quantum numbers n_1 and n_2 and by a magnetic quantum number m, which are related by

$$n_1 + n_2 + |m| = n - 1. \tag{2.7}$$

It is convenient to introduce an "electric" quantum number $k = n_2 - n_1$, which defines the projection of the dipole moment of an atom $e\mathbf{r}$ along the direction of an electric field **F**:

$$\langle n_1 n_2 m | e\mathbf{r}\mathbf{F} | n_1 n_2 m\rangle = eF\langle n_1 n_2 m | z | n_1 n_2 m\rangle = -\frac{3}{2} nkea_0 F. \tag{2.8}$$

The energy levels can be described, up to the second order in respect of the field intensity F, by the expression (in atomic units)

$$E = -\frac{1}{2n^2} - \frac{3}{2}Fnk - \frac{1}{16}F^2n^4(17n^2 - 3k^2 - 9m^2 + 19). \tag{2.9}$$

The parabolic wave functions $\Psi_{n_1n_2m}$ correspond to specific projections, along the direction of the electric field **F**, of the vectors representing the dipole **d** and orbital angular momenta **l** of an atom. The specific symmetry properties of the Coulomb field make it possible to express simply these parabolic functions in terms of spherical functions Ψ_{nlm} corresponding to specific values of l^2 and m^2 (see §37 in Ref. 1):

$$\Psi_{ni_1i_2} = \sum_{l=0}^{n-1} C(l,\ i_1 + i_2 | i_1,\ i_2)\,\Psi_{nlm}, \tag{2.10}$$

where $i_{1,2} = [m \pm (n_1 - n_2)]/2$; $C(l,m|l_1,l_2)$ are the Clebsch-Gordan coefficients.

The intensities I of the Stark components are described by matrix elements of the coordinate **r** of an atomic electron:

$$I(nn_1n_2m \to n'n_1'n_2'm') = \frac{4e^4\omega_0^4}{3c^3}\left|\langle nn_1n_2m|\mathbf{r}|n'n_1'n_2'm'\rangle\right|^2, \tag{2.11}$$

where ω_0 is the unperturbed frequency of the $n \to n'$ transition.

Depending on the polarization (linear, characterized by $\Delta m = 0$, or circular when $\Delta m = \pm 1$), the Stark component can be divided into π and σ. The intensities of the π components are governed by the matrix elements of the z component of **r** and the intensities of the σ components are determined by the x or y components of **r**. The general formulas for the matrix elements have been obtained by Gordon (see §65 in Ref. 1) and can be expressed in terms of the hypergeometric function

$$\Psi_m(n_i,\ n_i') = F\left(-n_i,\ -n_i',\ m+1, -\frac{4nn'}{(n-n')^2}\right). \tag{2.12}$$

In the case of the parabolic quantum numbers n_1 and n_2 (in contrast to the spherical quantum number l) there are no rigid selection rules for dipole radiation. Nevertheless, the distributions of the intensities of the Stark π and σ components obey certain relationships which we shall discuss later (Sec. 2.3). The Gordon formulas are very cumbersome and suitable only for calculations in few special cases (see Ref. 1). The formulas for the intensities expressed in terms of spherical coordinates can be simplified considerably in the semiclassical range.[20] Since the relationship between the parabolic and spherical bases is determined by the Clebsch-Gordan coefficients [see Eq. (2.10)] whose properties are known, we can expect to obtain satisfactory semiclassical expressions for the matrix elements also in terms of parabolic coordinates. However, such expressions have not yet been derived.

2.2 Radiative lifetimes of states

We shall now consider the simplest radiation parameter of the sublevels which is their lifetime governed by all possible radiative transitions to lower states.

The probability $A^{l}_{nn'}$ of radiative transitions and the lifetime T_{nl} of excited atomic states are usually analyzed using the spherical quantum numbers of atoms nl (see Ref. 1). Bureeva[19] obtained general semiclassical formulas for the calculation of the probabilities $A^{l}_{nn'}$ of radiative transitions. Goreslavskiĭ, Delone, and Kraĭnov[20] derived simple analytic expressions for $A^{l}_{nn'}$ which are highly accurate even when the numbers n and l are not too large. The structure of these expressions is related closely to the familiar formulas in the classical intensity of radiation in a Coulomb field (see §70 in Ref. 21). The quantum corrections to these probabilities can be found in Refs. 22 and 23.

Simple dependences of the probabilities A_{nl} on the orbital momentum l in the range $3 \leqslant n \leqslant 25$ are obtained in Ref. 24:

$$A^0(l) \approx A(1)\frac{1}{[1+\alpha(l-1)]^2}, \tag{2.13}$$

where the numerical coefficient α is selected so that it agrees with the exact result for $l = n - 1$:

$$\alpha = 0.7148 \pm 0.0004. \tag{2.14}$$

If we use the exact probability of a transition in the case when $l = n - 1$ (see Ref. 1), we obtain the following expression for $l > 0$:

$$A^0(l > 0) = 2.6759 \cdot 10^9\ \text{sec}^{-1} \times\left[\frac{1+\alpha(n-2)}{1+\alpha(l-1)}\right]^2 \frac{(2n-1)(2n^2-n-1)}{n^6(n-1)^2}. \tag{2.15}$$

Equation (2.15) ensures a high degree of accuracy so that the maximum deviations amount to a few percent in the range $l < n/2$.

If $l = 0$, the numerical results can be approximated satisfactorily by the formula[25]

$$A^0(0) \approx 5.97 \cdot 10^8\ \text{sec}^{-1}\frac{1}{n^2(n+1.46)}. \tag{2.16}$$

Following Herrick,[24] we shall describe the probability $B(nkm, n')$ of a transition from a parabolic state $|nkm\rangle$ to all the states of the level n':

$$B(nkm,\ n') = w(n,\ n') \sum_{k',\ m'} |\langle nkm|\mathbf{r}|n'k'm'\rangle|^2, \qquad (2.17)$$

where

$$w(n,\ n') = \frac{4e^2a_0^2}{3\hbar c^3}\left(\frac{1}{n^2} - \frac{1}{n'^2}\right)^3. \qquad (2.18)$$

Then, the total probability $B(k, m)$ of a transition from a given Stark sublevel to all the lower levels is

$$B(k,\ m) = \sum_{n'=|m|+1}^{n-1} B(nkm,\ n'). \qquad (2.19)$$

The corresponding lifetime is given by

$$\tau(nkm) = B^{-1}(k,\ m). \qquad (2.20)$$

The formulas (2.19) and (2.20) are "parabolic" analogs of the corresponding spherical quantities A_{nl} and $T_{nl} = A_{nl}^{-1}$. Using the familiar relationship between the parabolic and spherical functions given by Eq. (2.10), we obtain an expression relating the two types of probability:

$$B(k,\ m) = \sum_{l=|m|}^{n-1} A(n,\ l)\,[C(n,\ k|lm)]^2. \qquad (2.21)$$

It follows from the properties of the Clebsch-Gordan coefficients $C(n, k\,|lm)$ that the symmetry properties of the probabilities are

$$B(k,\ m) = B(-k,\ m) = B(k,\ -m). \qquad (2.22)$$

Summation over all the values of k and m clearly gives the total lifetime $A(n)$, which is independent of the summation bases:

$$A(n) = \sum_{k,\ m} B(k,\ m) = \sum_{l=0}^{n-1} (2l+1)\,A(n,\ l). \qquad (2.23)$$

An important sum rule is obtained from Eq. (2.21) by adding all the values of k and m in such a way that either $k + m$ or $k - m$ remains constant[24]:

$$n^{-1}A(n) = B(k,\ 0) + \sum_{m=1}^{(n-1-k)/2} B(k+m,\ m) + \sum_{m=1}^{(n-1+k)/2} B(k-m,\ m). \qquad (2.24)$$

If we sum in Eq. (2.24) the values of the number $k = n - 1$, $n - 3, \ldots, -(n-1)$ over all n, we again obtain Eq. (2.23).

It follows from Eq. (2.24) that the distribution of the transition probabilities in the $m = 0$ case is determined uniquely by the distributions $B(k, m)$ when $m \neq 0$. The latter are found to depend weakly on the "electric" quantum number k. It is therefore convenient to introduce average (in terms of "k") values of $B(k, m)$ described by

$$\overline{B}(m) = \frac{1}{n-|m|}\sum_{k} B(k,\ m) = \frac{1}{n-|m|}\sum_{l=|m|}^{n-1} A(n,\ l). \qquad (2.25)$$

Since in the $m \neq 0$ case we can quite accurately assume that $B(k, m) = \overline{B}(m)$, we can obtain $B(k, 0) \approx B^0(, 0)$ from Eq. (2.24), which gives

$$B^0(k,\ 0) = n^{-1}A(n) - \sum_{m=1}^{(n-1-k)/2} \overline{B}(m) - \sum_{m=1}^{(n-1+k)/2} \overline{B}(m). \qquad (2.26)$$

If $k = n - 1$, this relationship reduces to

$$B^0(n-1,\ 0) = n^{-1}A(n) - \sum_{m=1}^{n-1} \overline{B}(m). \qquad (2.27)$$

In the range of lower values $k < n - 1$ the quantities $B^0(k,0)$ are found from the recurrence relationship

$$B^0(k-2,\ 0) = B^0(k,\ 0) - \overline{B}\left(\frac{n+1-k}{2}\right) + \overline{B}\left(\frac{n-1+k}{2}\right). \qquad (2.28)$$

The quantities $\overline{B}(m)$ can be found from Eq. (2.25) by means of the approximate expressions given in Eq. (2.13) for $A(n,l)$:

$$\overline{B^0}(m) = \frac{A^0(m)}{n-m} + \frac{A^0(1)}{n-m}\,\frac{n-1-m}{\{1+\alpha[m-(1/2)]\}\{1+\alpha[n-(1/2)]\}}, \quad m > 0. \qquad (2.29)$$

A comparison of the results for $\overline{B}(m)$ and $B(k, 0)$ based on the use of the approximation represented by Eqs. (2.28) and (2.29) with the results of exact calculations is made in Table I. It is clear from Table I that these approximations are quite accurate. Therefore, the method described above makes it possible to determine the lifetime $B(k, m)$ of the Stark sublevels of the hydrogen atom using simple analytic formulas and thus avoid direct summation of the series in Eq. (2.21) containing the Clebsch-Gordan coefficients.

2.3. Intensities of Stark components

The intensities of the Stark components are described by the general Gordon formulas (see Ref. 1) for the matrix elements of the components of the radius vector of an atomic electron expressed in parabolic coordinates. However, the application of these formulas involves very time-consuming numerical calculations, particularly in the case of highly excited levels. The situation is also complicated by the absence of rigorous selection rules for the parabolic quantum numbers.

In the case of large values $n \gg 1$ we can establish simple relationships governing the distributions of the intensities of the components in the case of transitions characterized by a small change in the quantum number $n - n' \equiv \Delta n \ll n$ which are of practical interest. Following Gulyaev,[14,26] we shall consider these relationships in the case of highly excited lines $H_{n\alpha}$ ($\Delta n = 1$) and $H_{n\beta}$ ($\Delta n = 2$) observed under astrophysical conditions.

The change $\Delta\omega$ in the frequency of a transition in an electric field F corresponding to the Stark component $n_1n_2m \to n_1'n_2'm'$, is—according to Eq. (2.9)—given by

$$\frac{\Delta\omega}{\omega_F} = n(n_1 - n_2) - n'(n_1' - n_2'), \quad \omega_F \equiv \frac{3}{2}\frac{ea_0}{\hbar}F. \qquad (2.30)$$

The intensities of the components are sensitive functions of the combinations of quantum numbers $K \equiv (n_1 - n_2) - (n_1' - n_2') = k - k'$ and $i \equiv n_1' - n_2' \equiv k'$, where $\Delta\omega$ becomes

$$\frac{\Delta\omega}{\omega_F} = Kn + \Delta n \cdot i. \qquad (2.31)$$

The parameter K, which ranges from $-(2n - 2 - \Delta n)$ to $(2n - 2 - \Delta n)$, groups the components of $2(2n - 2 - \Delta n)$ series, each of which contains $2(n - \Delta n) - (K + 1)$ terms labeled by the parameter i. Figures 2 and 3 show the grouping of the components in the case of the $H_{5\alpha}$ and $H_{5\beta}$ and

TABLE I. Comparison of probabilities of radiative $\overline{B}(i)$ and $B(i, 0)$ transitions obtained using approximation formulas (2.28) and (2.29) (columns denoted by A) with exact results[25] (columns denoted by B) for $n = 10$ Level of hydrogen (Ref. 24).

i	$B(i)$		$B(i, 0)$	
	A	B	A	B
1	1,0905	1,0871	0,4753	0,4806
2	0,5472	0,5523		
3	0,3623	0,3658	0,5666	0,5685
4	0,2703	0,2722		
5	0,2155	0,2163	0,7757	0,7706
6	0,1791	0,1794		
7	0,1532	0,1532	1,1891	1,1733
8	0,1338	0,1338		
9	0,1186	0,1188	2,1610	2,1473

$H_{6\beta}$ lines. We can see that the parity (or nonparity) of the number of K corresponds to the σ (or π) polarization of the components of the lines H_α and H_β. The separation between the components within the series $\Delta\omega_i$ and the separation $\Delta\omega_k$ between the centers of the series are

$$\Delta\omega_i = \omega_F \Delta n, \quad \Delta\omega_k = \omega_F n = \frac{\Delta\omega_i n}{\Delta n}. \tag{2.32}$$

We shall now consider the nature of changes in the intensity on increase in the number K. We shall utilize the fact that arguments of the hypergeometric functions in Eq. (2.12), which occur in the Gordon formulas,[1] are large if $1 \sim \Delta n \ll n \sim n'$ so that these functions can be replaced by the last (largest) terms:

$$\Psi_m(n_i, n_i') \approx \frac{n_i'!m!}{(n_i'-n_i)!\,(m+n_i)!}\, b^{2n_i}(-1)^{n_i}, \tag{2.33}$$

where $b = 4nn'/(n-n')^2 \gg 1$ (to be specific, we shall assume that $n_i' \gtrsim n_i$ and instead of $|m|$ we shall write simply m).

The approximation of Eq. (2.33) allows us to obtain simple analytic expressions for the matrix elements of the coordinate governing the intensities of the π and σ components. We shall consider specific transitions characterized by $\Delta n = 1$ ($H_{n\beta}$ lines) and $\Delta n = 2$ ($H_{n\beta}$ lines).

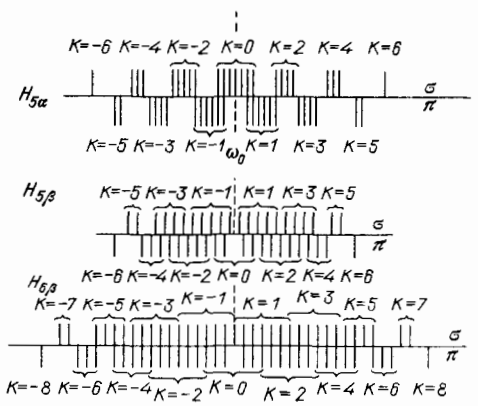

FIG. 2. Stark splitting of the $H_{5\alpha}$ lines, belonging to the Brackett series, and of $H_{5\beta}$ and $H_{6\beta}$ lines.[14,26] The upper rows of lines are the σ components and the lower rows are the π components.

2.3.1. $H_{n\alpha}$ lines (transitions with $\Delta n = 1$)

The central series ($K = 0$) is formed by the σ components and the transitions in this case are described by the relationships

$$\begin{aligned} &n_1 = n_1', \quad n_2 = n_2' \quad \text{for} \quad m \to m-1, \\ &n_1 = n_1'+1, \quad n_2 = n_2'+1 \quad \text{for} \quad m \to m+1. \end{aligned} \tag{2.34}$$

The next series ($K = \pm 1$) represents the components for which the similar conditions are

$$\begin{aligned} &n_1 = n_1'+1, \quad n_2 = n_2' \quad \text{for} \quad K = +1, \\ &n_1 = n_1', \quad n_2 = n_2'+1 \quad \text{for} \quad K = -1. \end{aligned} \tag{2.35}$$

Using the approximation of Eq. (2.33) and the relationships given by Eqs. (2.34) and (2.35), we find from the Gordon formulas the following simple expressions for the matrix elements

$$x_m^{m-1} = \frac{a_0}{4} b\,[(n_1+m)(n_2+m)]^{1/2}\left[1 - \frac{(n_1+1)(n_2+1)}{b^2}\right], \tag{2.36}$$

$$x_m^{m+1} = \frac{a_0}{4} b\,(n_1 n_2)^{1/2}\left[1 - \frac{(n_1+m)(n_2+m)}{b^2}\right], \tag{2.37}$$

$$z_m^m = \frac{a_0}{4} b\,\{[n_1(n_1+m)]^{1/2}\delta_{K,+1} + [n_2(n_2+m)]^{1/2}\delta_{K,-1}\}. \tag{2.38}$$

The fall of the intensity on increase of the number K is described by the ratio

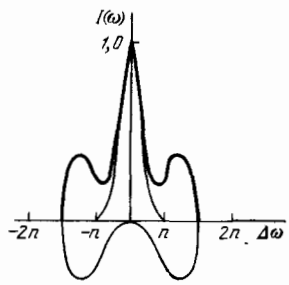

FIG. 3. Distribution of the intensity $I(\omega)$ plotted as a function of the frequency shift $\Delta\omega$ [in units of $(3/2)ea_0F/\hbar$] for $H_{n\alpha}$ lines characterized by $n \gg 1$ (Refs. 14 and 26). The thin lines are the envelopes of the σ (top part) and π (lower part) components and the thick line is the combined line profile.

$$\frac{[(x_m^{m+1})^2+(x_m^{m-1})^2]_{K+2}}{[(x_m^{m+1})^2+(x_m^{m-1})^2]_K} \approx \frac{n_1(n_1+m)\,n_2(n_2+m)}{b^4}, \qquad (2.39)$$

which cannot exceed $2^{-8}\sim 4\times 10^{-3}$ (a similar estimate applies also to z_m^m). Therefore, there is practical interest only in the nearest σ and π series, corresponding to the first few values of K).[1)]

We can calculate the intensity of a line shifted by $\Delta\omega = \omega_F(Kn+i)$ by summing the squares of the matrix elements allowing for the remaining degeneracy in respect of m. In the case of the central σ series ($K=0$) and a given value of i, such summation yields

$$I_i^\sigma \propto \sum_m [(x_m^{m-1})^2+(x_m^{m+1})^2] \approx \frac{a_0^2}{24} n^2(2n^3-3n^2i+i^3). \qquad (2.40)$$

Similarly in the case of the nearest π series ($K=1$), we find that

$$I_i^\pi \propto \sum_m (z_m^m)^2 \approx \frac{a_0^2}{24} n^2(n^3+3n^2i-3ni|i|-i^2|i|). \qquad (2.41)$$

Figure 3 shows schematically the splitting of the $H_{n\alpha}$ line in the case when $n\gg 1$.

The central σ ($K=0$) series, the nearest π series ($K=\pm 1$), and the distribution of the total (summed over K) intensity are shown in the figure. The intensity of the σ series decreases by half when the width $\Delta\omega_{1/2} = (n/3)\omega_F$ is reached. The intensity minimum in the π series corresponds to $4\Delta\omega_{1/2}$ and represents approximately 40% of the maximum intensity of the central σ series.

2.3.2. $H_{n\beta}$ lines (transitions with $\Delta n=2$)

In the case of the odd n the components of the π series of these lines never coincide with the components of the σ series (Fig. 2). Beginning from the $H_{6\beta}$ line, the terms of the series with $K=+1$ and -1 corresponding to the σ polarization begin to overlap. This overlap is the reason for the nonzero intensity at the line center ($\Delta\omega=0$) because the intensity of the π components of the central ($K=0$) series vanishes for $\Delta\omega=0$.

If we follow the procedure used above for the $H_{n\alpha}$ line, we can calculate consecutively the intensities of the series $I_{\pi_0}(K=0, \Delta m=0)$, $I_{\sigma_1}(K=\pm 1, \Delta m=\pm 1)$, $I_{\pi_2}(K=\pm 2)$, etc. The structure of the $H_{n\beta}$ lines is shown in Fig. 4, which gives also the separate contributions of the π and σ series.[2)] The positions of the line maxima correspond to frequencies obeying $\Delta\omega_n = \pm 1.6n'$. Their width at mid-amplitude amounts to $2.85n\omega_F$. The intensity at the center is 13% of $I_{\max}$ irrespective of the value of n. The line half-width is $\Delta\omega_{1/2} = 3.6\omega_F$.

2.4. Weak fields. Asymptotic theory of decay of an atom

The behavior of an atom in an electric field F depends on the ratio of F to the critical intensity $F_c \propto 1/16n^4$ [see Eq. (1.4)] at which the barrier along the coordinate η disappears for a given level n and the classical above-barrier motion of an electron becomes possible (Fig. 1). If $F \ll F_c$, the barrier width is fairly wide and the energy levels of an electron are well localized, i.e., the level width Γ is exponentially small. This case was treated by Smirnov and Chibisov[27] who developed an asymptotic method for the calculation of the atomic parameters. Damburg and Kolosov[28] suggested a method based on the similarity of decay to the scattering of an electron by a quasidiscrete level. In both cases we are dealing with a resonance energy level lying against the background of a continuous spectrum (continuum). When the electron energy E approaches the energy of a discrete level E_0, the phase φ of the wave function changes abruptly[3)]:

$$\varphi = \varphi_0 + \operatorname{arctg}\frac{\Gamma}{2(E-E_0)}. \qquad (2.42)$$

Having determined the wave function, we can then find the parameter Γ and the value of E_0 from Eq. (2.42).

Determination of the wave function of an atomic electron in the limit of weak fields F is based in Ref. 28 on the matching of solutions at low and high values of the coordinate η (along which an electron can reach the continuum).

The details of the method are described fully in the review of Damburg and Kolosov (see Ref. 17, p. 31). The result is

$$\Gamma = (4R)^{2n_1+m+1}e^{-2R/3} \times [n^3 n_2!\,(n_2+m)!]^{-1}, \qquad (2.43)$$

where $R = (-2E_0)^{3/2}/F$. Equation (2.43) was first derived in Ref. 27, but there E was assumed to be the unperturbed value. In fact, terms of the order of F in the expansion for the energy are important in the argument of the exponential function, whereas terms of higher order occur in the correction terms. Refs. 17, 27, and 28 give the results of an expansion of Γ right up to terms of the order of F^2. The results of this asymptotic theory are in good agreement with the numerical calculations carried out for fields of intensities $F \ll F_c$ (see Refs. 17 and 28).

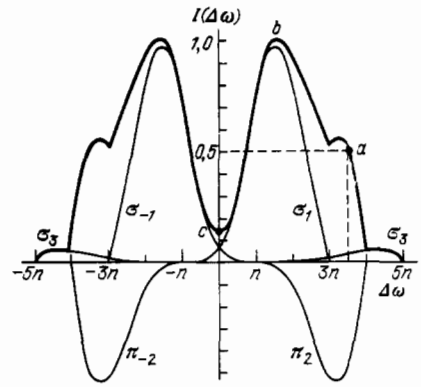

FIG. 4. Structure of the $H_{n\beta}$ lines in the $n\gg 1$ case.[14,26] The notation is the same as in Fig. 3. Points: a) level corresponding to half-intensity $I_{\max}/2$; b) maximum intensity; c) central dip.

2.5. Classical theory of decay of an atom in an electric field

An increase in the electric field F reduces the effective potential barrier V_η along the coordinate η. In the case of highly excited states of an atom we can have a situation when an energy level coincides with the maximum of the potential barrier, i.e., when $E_c = V_{\eta\max}$ (Fig. 1). This critical energy corresponds to a critical electric field F_c in which two points of intersection of the straight line $V_\eta = E$ with the potential V_η coincide (roots η_2 and η_3 in Fig. 1 merge). In this case above-barrier emission of an electron from an atom is clearly possible and it is allowed by the laws of classical mechanics. Hence, obviously the critical values E_c and F_c can be found by purely classical calculations. This was done by Banks and Leopold[31] and we shall follow their treatment below.

The separation of variables in terms of the parabolic coordinates ξ and η of an electron in a Coulomb field e^2/r and in an external field F makes it possible to treat the motion of an electron in effective potentials of Eq. (2.3), as shown already in Sec. 2.1.

It is convenient to introduce momenta p_η and p_ξ for each variable η and ξ, defined by

$$\frac{p_\xi^2}{2m} + V_\xi(\xi) = E, \quad \frac{p_\eta^2}{2m} + V_\eta(\eta) = E, \tag{2.44}$$

where E is the total energy of an electron in an atom. In the case of bound states the value of E lies within the range (Fig. 1)

$$\max(V_{\xi\min}, V_{\eta\min}) \leqslant E \leqslant V_{\eta\max} \leqslant 0. \tag{2.45}$$

In the case of this value of E the points of intersection of the straight line $E = \text{const}$ with the curves representing the effective potential V_ξ and V_η are described by cubic equations with three roots each: $\xi_1, \xi_2, -\xi_3, \eta_1, \eta_2$, and η_3.

Our task is to find the dependences of the critical parameters E_c and F_c on the classical action variables I_φ, I_ξ, and I_η, representing the state of an electron in an atom. It is convenient to derive this dependence in a parametric form by expressing all the dependences in terms of the roots of the equations $V_\xi = E$ and $V_\eta = E$ and then requiring that the roots $\eta_2 = \eta_3$ coincide for the critical values of the parameters E_c and F_c.

The expressions for the classical action variables I_ξ and I_η, expressed in terms of the roots ξ_i and η_i are

$$I_\xi = \frac{1}{2\pi}\oint p_\xi\,d\xi = \frac{(2meF)^{1/2}}{\pi}\int_{\xi_1}^{\xi_2}[(\xi_2-\xi)(\xi-\xi_1)(\xi+\xi_3)]^{1/2}\frac{d\xi}{\xi}, \tag{2.46}$$

$$I_\eta = \frac{1}{2\pi}\oint p_\eta\,d\eta = \frac{(2meF)^{1/2}}{\pi}\int_{\eta_1}^{\eta_2}[(\eta_2-\eta)(\eta-\eta_1)(\eta_3-\eta)]^{1/2}\frac{d\eta}{\eta}, \tag{2.47}$$

$$I_\varphi = \text{const}. \tag{2.48}$$

The formulas (2.46)–(2.48) together with the equations for the roots and the condition $\eta_2 = \eta_3$ yield a parametric relationship between the critical parameters E_c and F_c and the action variables. This relationship can be written in the form

$$F_c = \frac{m^2e^5}{I^4}\Phi_c(u, v), \tag{2.49}$$

$$E_c = -\frac{me^4}{2I^2}\mathscr{E}_c(u, v), \tag{2.50}$$

where we have introduced the total action $I = I_\xi + I_\eta + I$ and the parameters $u = I_\eta/I$ and $v = I_\xi/I$, the values of which lie in a triangular region defined by

$$\Delta\{u \geqslant 0,\ v \geqslant 0,\ u + v \leqslant 1\}. \tag{2.51}$$

The functions $\Phi_c(u, v)$ and $\mathscr{E}_c(u, v)$ are generally found by numerical solution of the above equations. In the most interesting limiting cases the classical values of the critical parameters are

$$\begin{aligned} &n^4F_c = \frac{2^{10}}{3^4\pi^4} = 0.13, \quad |E_c|n^2 = \frac{2^6}{3^2\pi^2} = 0{,}72 \quad \text{for} \quad n_1 = n,\\ &n^4F_c = 0.3834, \qquad\qquad E_c = 0 \quad \text{for} \quad n_2 = n,\\ &n^4F_c = \frac{2^{12}}{3^9} = 0.208, \quad |E_c|n^2 = \frac{2^7}{3^5} = 0{,}527 \quad \text{for} \quad m = n. \end{aligned} \tag{2.52}$$

This classical method for the calculation is effective when estimates are being obtained of the ionization of an atom from highly excited states $n \gg 1$ and $l \gg 1$, and the general quantum-mechanical theory meets with considerable computational difficulties. The critical values of the parameters given in Eq. (2.52) are in good agreement with the values found by quantum calculations in the relevant range of the parameters (see Sec. 2.6 below).

2.6. Decay of states near the critical value of an electric field

The classical results obtained in Sec. 2.5 for the characteristics of an atom in an electric field F can be generalized allowing for the quantum (tunnel) effects in the semiclassical approximation. According to the Bohr-Sommerfeld rules, the values of the action variables (2.46) and (2.47) are related to the parabolic quantum numbers by

$$I_\xi = \pi\left(n_1 + \frac{1}{2}\right), \quad I_\eta = \pi\left(n_2 + \frac{1}{2}\right). \tag{2.53}$$

The conditions of Eq. (2.53) have been used frequently in the literature (see Ref. 17). For example, Zaretskiĭ and Kraĭnov[32] used the relationships in Eq. (2.53) to find the behavior of an atom in a low frequency electric field. Kadomtsev and Smirnov[33] investigated the atomic parameters near the critical field F_c.

We shall find, following Ref. 33, the field F_c which suppresses the barrier and we shall do this employing the semiclassical quantization conditions given by Eq. (2.53), Eqs. (2.1) and (2.2), and the additional condition

$$\left.\frac{dp_\eta}{d\eta}\right|_{\eta=\eta_2} = 0, \tag{2.54}$$

where p_η is the momentum of an electron in the η space and η_2 is the right-hand turning point which coincides (when $F = F_c$) with the maximum of the effective potential energy. These equations establish a unique relationship between the separation constants β_1 and β_2, the electron energy E, and the critical field intensity F_c.

The solution of this system of equations is simplest in the case when $m = 0$. For example, in the limit $n_2 \to 0$, the solution gives[33]

$$F_cn^4 = \frac{2^{10}}{3^4\pi^4}\left(1 + 0.4\,\frac{n_2}{n}\right), \quad |E_c|n^2 = \frac{2^7}{3^2\pi^2}\left(1 - 0.4\,\frac{n_2}{n}\right). \tag{2.55}$$

We can see that the zeroth order terms of the expansion coincide exactly with the results of a classical analysis of Eq. (2.52). In the limit $n_2 \to 0$, we find that

$$F_cn^4 \approx 0.383\left[1 - 1.75\left(\frac{n_2}{n}\right)^{2/3}\right]^6, \quad \frac{n_2}{n} \ll 1, \tag{2.56}$$

$$|E_c|n^2 \approx 1.48\left(\frac{n_1}{n}\right)^{2/3}\left[1 - 1.1\left(\frac{n_2}{n}\right)^{2/3}\right]^2. \tag{2.57}$$

In the limiting case these results also agree with Eq. (2.52). The correction factors given in the square brackets

were obtained by Drukarev[18] (see also Sec. 2.7).

The solution of the system of semiclassical equations is fairly cumbersome in the general case when $m \neq 0$ and it was obtained numerically in Ref. 32. In the case when $m = n$ the results of the semiclassical analysis reduce to those given by the classical formulas (2.52).

We can now plot the critical fields F_c and the corresponding energies $|E_c|$ throughout the plane of the variables n_1 and n_2 (Fig. 5). The corresponding classical results of Eq. (2.52) are located at the corners of the triangles in Fig. 5 in the region of $n \approx n$ (if $n \approx m$).

This method allows us to calculate the rate of decay Γ of an atom near the critical field $|F - F_c| \ll F_c$.

The calculations reported in Ref. 33 are based on the approximation of a barrier near its maximum by a parabola, followed by determination of the above-barrier transmission coefficient. We shall not consider details, but simply give the rate of decay Γ for $F = F_c$ and $n_2 = n$:

$$\Gamma \approx \frac{1}{3.27 n^3 \ln (3\pi n/4)}. \tag{2.58}$$

We can see that the rate of decay is not exponentially small (in contrast to the case when the field is weak $F \ll F_c$) and, moreover, it is comparable with the period of motion of an electron along an orbit.

It is interesting to estimate the ratio of the width Γ of a level to its energy E_c at the critical point. According to Eqs. (2.57) and (2.58), we have

$$\frac{\Gamma}{E_c} = \frac{1}{2.35 n \ln (3\pi n/4)} \ll 1. \tag{2.59}$$

Therefore, the ratio of the indeterminacy of the energy of a level to the energy itself amounts to 1.8×10^{-3} for $n = 50$ and 5.5×10^{-3} for $n = 20$.

2.7. Semiclassical theory of atomic states in an electric field

2.7.1. Basis of the semiclassical approach

We shall consider a more general semiclassical theory of decay of levels in an electric field, which makes it possible to follow the smooth transition from the case of weak fields $F \ll F_c$ to fields which are comparable with the critical value. It should be pointed out that although the fundamentals of the semiclassical theory were provided by Lanczos[34] back in the thirties, specific calculations have largely remained incomplete. Such calculations have been carried out recently, as pointed out above, using more rigorous methods (see Refs. 17, 18, 31, and 32). We shall follow the results of Drukarev[18] who carried out a consistent calculation of the energies and widths of levels by the semiclassical method.

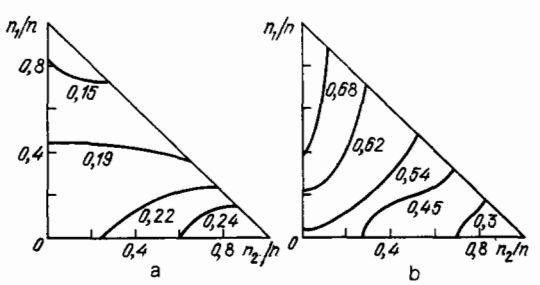

FIG. 5. Reduced values of the critical electric field $F_c n^4$ (a) and of the level energy En^2 (b) plotted in the plane of the quantum numbers n_1 and n_2 (Ref. 33).

The semiclassical theory is based on the quantization rules given by Eqs. (2.46)–(2.48) and (2.53). If the relevant numbers are sufficiently small so that $|m|/|n| \ll 1$ the integrals of Eqs. (2.46) and (2.47) can be represented in the form

$$L_1(x_1) = \frac{1}{2}\int_0^{x_1}\left(-1 + \frac{4\alpha_1}{x} - wx\right)^{1/2} dx = \left(n_1 + \frac{|m|+1}{2}\right)\pi, \tag{2.60}$$

$$L_2(y_1) = \frac{1}{2}\int_0^{y_1}\left(-1 + \frac{4\alpha_2}{y} + wy\right)^{1/2} dy = \left(n_2 + \frac{|m|+1}{2}\right)\pi, \tag{2.61}$$

where we shall use the notation of Eqs. (2.5) and (2.6) for the separation constants α_1 and α_2 and for the field w.

In this approximation the energy E (or the effective principal quantum number ν) are functions of two parameters:

$$S = \frac{n_1 - n_2}{n}, \quad T = 4n^4 F. \tag{2.62}$$

We shall find ν by noting that the integrals of Eqs. (2.60) and (2.61) can be expressed in terms of the hypergeometric function $F(-1/2, 1/2, 2, +z) \equiv F(+z)$, so that

$$L_1 = \pi\alpha_1 (1 - z_1) F(-z_1), \quad L_2 = \pi\alpha_2 (1 + z_2) F(z_2), \tag{2.63}$$

where

$$z_1 = \frac{(1+16\alpha_1 w)^{1/2} - 1}{(1+16\alpha_1 w)^{1/2} + 1}, \quad z_2 = \frac{1 - (1-16\alpha_2 w)^{1/2}}{1 + (1-16\alpha_2 w)^{1/2}}. \tag{2.64}$$

Using the quantization conditions of Eqs. (2.60) and (2.61), we obtain

$$\alpha_1 = \frac{n_1 + (1/2)(|m|+1)}{(1-z_1)^{1/2} F(-z_1)}, \quad \alpha_2 = \frac{n_2 + (1/2)(|m|+1)}{(1+z_2)^{1/2} F(z_2)}. \tag{2.65}$$

Hence, it is clear that

$$\alpha_1 \geqslant n_1 + \frac{|m|+1}{2}, \quad \alpha_2 \leqslant n_2 + \frac{|m|+1}{2}. \tag{2.66}$$

We shall next express $\alpha_1 w$ and $\alpha_2 w$ in terms of z_1 and z_2 using Eqs. (2.64) and substitute expressions from Eq. (2.65) for α_1 and α_2, which yields

$$\left(n_1 + \frac{|m|+1}{2}\right) w = \frac{z_1}{4(1-z_1)^{3/2}} F(-z_1), \tag{2.67}$$

$$\left(n_2 + \frac{|m|+1}{2}\right) w = \frac{z_2}{4(1+z_2)^{3/2}} F(z_2). \tag{2.68}$$

It follows from the last relationship that the maximum value is attained at $z_2 = 1$ and it is

$$w_c = \left[3\pi\sqrt{2}\left(n_2 + \frac{|m|+1}{2}\right)\right]^{-1}. \tag{2.69}$$

The value w_c clearly determines the critical field F_c and we can find this field if we know the energy E (parameter ν).

If we use Eq. (2.69), we can reduce Eq. (2.68) to

$$\frac{w}{w_c} = \frac{3\pi\sqrt{2}}{4} \frac{z_2}{(1+z_2)^{3/2}} F(z_2). \tag{2.70}$$

2.7.2. Energy levels

We shall now find the equations for the determination of the effective principal quantum number $\nu = (-2E)^{1/2}$. We shall do this using the relationship $\alpha_1 + \alpha_2 = \nu$ between the separation constants in Eqs. (2.65), which yields the relationship between ν/n and the parameter S [Eq. (2.62)] and the variables z_1 and z_2 [Eq. (2.64)].

The relationships (2.67) and (2.68) then give two other equations relating the parameters T, S, and ν to the combinations of the functions $F(-z_1)$ and $F(z_2)$. These three equations and simple transformations yield the parametric relationship between ν/n and the parameters S and T (Ref. 18):

$$\frac{\nu}{n} = \frac{\nu}{n}(z_1, z_2),$$
$$S = S(z_1, z_2), \quad T = T(z_1, z_2). \tag{2.71}$$

The procedure of finding ν with the aid of the system of equations (2.71) reduces to the following: given S and T, we use Eq. (2.7) to find z_1 and z_2; substituting them in the expression for ν/n, we then find the required quantity. In general, this procedure is carried out numerically. In Ref. 18 the dependences of z_1 and z_2 on T were reported for different values of S. Some of the numerical data on the parameter ν/n can be found in Table II.

We shall now compare the results of the semiclassical theory [Eq. (2.71)] with those obtained by classical calculations [Eq. (2.52)] in the case when $m = 0$, $n_2 = n$, and $F = F_c$ (see Ref. 18). We shall do this by assuming that the parameter z_2 in Eq. (2.71) is unity, which corresponds [according to Eq. (2.64)] to the critical value $F = F_c$ ($w = w_c$). Bearing in mind that $F(z_2 = 1) = 8/3\pi$ is given by Eq. (2.71), we obtain $\nu/n = 3\pi \times 2^{-7/2}$ and hence the energy $E = -\nu^{2/2}$ is exactly equal to the classical value of Eq. (2.52). Using then Eq. (2.69), we find the critical field $F_c = w_c \nu^{-3}$, we can see that is also agrees with the classical estimate of Eq. (2.52).

2.7.3. Decay rates

A calculation of the rate of decay Γ in Ref. 18 is based on finding the asymptotic form of the wave function based on the semiclassical method.[35] Determination of the asymptote of the semiclassical function is related to the problem of determination of the penetrability of the potential barrier $V(y)$ in the y space. This problem can be solved exactly either for a barrier of parabolic shape or in the limiting case of low penetrability (large width) of the barrier. In our case the barrier shape is nearly parabolic near its top, far from the top the penetrability is weak. Consequently, we can derive a single analytic expression which is approximately valid for any barrier penetrability.

If K and Φ are the parameters governing the penetrability and the phase of the wave function,

$$K = \int_{y_1}^{y_2} p(y)\,dy, \quad \Phi = \int_{y_{\min}}^{y_1} p(y)\,dy + \delta(K), \tag{2.72}$$

where $y_{1,2}$ are the turning points to the left and right of the barrier [$p(y)$ is the momentum in the y space], an approximate expression for Γ becomes

$$\Gamma \approx e^{-2K}\left[2\left(\frac{d\Phi}{dE}\right)_{E_n}\right]^{-1}. \tag{2.73}$$

The physical meaning of Eq. (2.73) is clear: the rate of decay Γ is proportional to the frequency of motion of an electron in a potential well $(d\Phi/dE)_{E_n}^{-1}$ multiplied by the decay probability e^{-2K} on approach to the barrier. Both these parameters can be expressed, by analogy to Sec. 2.7.1, using analytic functions $h(z_2)$ and $g(z_2)$ related to the hypergeometric functions

$$\Gamma = \frac{\exp[-g(z_2)/w]}{\nu^3 h(z_2)}. \tag{2.74}$$

The general form of the functions h and g can be found in Ref. 18. In the case of weak fields $F \ll F_c$ we can use the relationship (2.64) between the parameter z_2 and the field w, which readily yields an asymptotic expression for the decay parameter Γ which is identical, as expected, with the results of the asymptotic theory.

When the field F is close to the critical value F_c ($F_c - F \ll F_c$), the parameter z_2 is close to unity: $1 - z_2 \ll 1$. We then have

$$g(z_2) \approx \frac{\pi}{2^{1/6} \cdot 16}(1 - z_2)^2. \tag{2.75}$$

The limiting value of the function $h(1)$ is

$$h(1) = \sqrt{2}\left[6 - \ln(32\sqrt{2}\,w_c) - \Psi\left(\frac{1}{2}\right)\right] \tag{2.76}$$

(Ψ is the logarithmic derivative of the Γ function). It is interesting to compare the value of Γ at the point $F = F_c$ with the results given by Eq. (2.58) in Sec. 2.6. Substituting Eqs. (2.75) and (2.76) into Eq. (2.74), we find that the two results for the line width diverge by a factor of about 2.5. This divergence may be entirely due to the difference between the analytic approximations (see Ref. 18).

A comparison of the results of the semiclassical theory[18] for the parameters ν and Γ with the quantum-mechanical calculations[28] is made in Table II (based on Ref. 18).

2.8. Results of numerical calculations

Numerical calculation methods have been developed in several papers [29,36–38] and their results agree generally quite well with one another but they differ considerably from the

TABLE II. Comparison of quantum-mechanical[28] and semiclassical[18] calculations.

n, F	ν		Γ, 10^{-6} sec^{-1}	
	Ref. 28	Ref. 18	Ref. 28	Ref. 18
$n=5$, $F=1{,}8\cdot10^{-4}$	4,9240	4,929	2,282	2,55
$n=11$, $F=10^{-5}$	10,6882	10,722	2,815	3,3
$n=15$, $F=3\cdot10^{-6}$	14,5771	14,619	1,338	1,74

results of calculations carried out using the earlier method of Lanczos (see Ref. 17). The numerical results can be represented conveniently (for many of their applications) in a semianalytic form based on perturbation theory in respect of the field.[37] The energies $E(n_1,n_2,m,\lambda)$ and the widths $\Gamma(n_1,n_2,m,\lambda)$ of Stark sublevels can be written in the form of power series in terms of the parameter $\lambda = n^3F/4$:

$$E(n_1,\ n_2,\ m,\ \lambda) = -\frac{1}{2n^2}\left(1+4\sum_p c_p(n_1,\ n_2,\ m)\,\lambda^p\right), \tag{2.77}$$

where the coefficients c_p are found by perturbation methods.[37] The first three coefficients are described by

$$c_1 = -3(n_1-n_2),\quad c_2 = \frac{1}{2}[17n^2-3(n_1-n_2)^2-9m^2+19],$$
$$c_3 = -3(n_1-n_2)[23n^2-(n_1-n_2)^2+11m^2+39]. \tag{2.78}$$

The first two correspond clearly to the familiar linear and quadratic Stark effects. The coefficients c_p are given right up to the ninth order[4)] in Ref. 37.

Analytic expressions for the widths Γ of levels are closely related to the frequency of motion of an electron in a potential well governed by the derivative $\partial E/\partial n_2$:

$$\Gamma(n_1,\ n_2,\ m,\ \lambda)$$
$$= \frac{1}{2\pi}\frac{\partial E(n_1,\ n_2,\ m,\ \lambda)}{\partial n_2}\exp[-K(n_1,\ n_2,\ m,\ \lambda)]. \tag{2.79}$$

The function $K(n_1,n_2,m,\lambda)$ clearly describes the barrier penetrability. The derivative $\partial E/\partial n_2$ is found by differentiating the series of Eq. (2.77).

The function K describing the barrier penetrability can be found using an asymptotic series for Γ of the type (see Sec. 2.4)

$$\Gamma(n_1n_2m\lambda) = \frac{\exp[3(n_1-n_2)-(1/6\lambda)]}{n^3n_2!\,(n_2+m)!\,\lambda^{2n_2+m+1}}\sum_{k\geqslant 0} a_k(n_1n_2m)\,\lambda^k, \tag{2.80}$$

where the coefficients $a_k(n_1n_2m)$ are expressed in terms of the coefficients of Eq. (2.77) using the dispersion relationship

$$c_p(n_1n_2m) = \frac{n^2}{4\pi}\int_0^{+\infty}[\Gamma(n_1n_2m\lambda)+(-1)^p\,\Gamma(n_1n_2m\lambda)]\,\frac{d\lambda}{\lambda^{p+1}}. \tag{2.81}$$

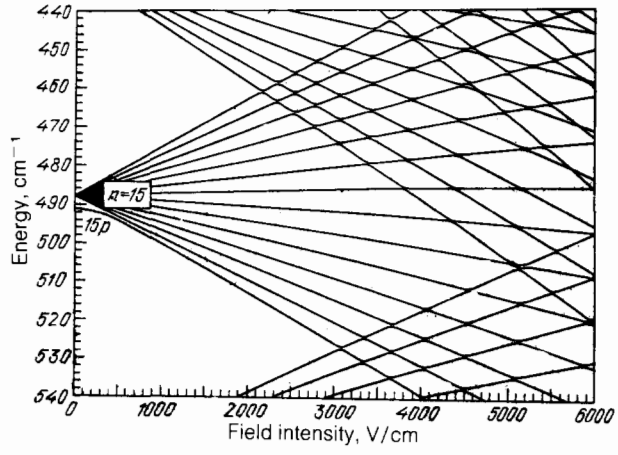

FIG. 6. Stark splitting of a highly excited lithium atom.[38]

The relationship (2.81) is deduced from the condition of analyticity of the energy in the plane of complex values of the field F (for details see Ref. 37, p. 328).

A comparison of the coefficients a_k with the coefficients c_p from Eq. (2.81) makes it possible to obtain the following relationship for the function K:

$$K(n_1n_2m\lambda) = (6\lambda)^{-1} + \ln[\lambda^{2n_2+m+1}n_2!\,(n_2+m)!\,(2\pi)^{-1}]$$
$$+3(n_2-n_1)$$
$$-\frac{1}{6}\int_0^{\lambda}\left[n^3\frac{\partial E(n_1n_2m\lambda')}{\partial n_2}-1\right.$$
$$\left.+6(2n_2+m+1)\,\lambda'\right]\frac{d\lambda'}{\lambda'^2}. \tag{2.82}$$

It therefore follows that the coefficients c_p tabulated in Ref. 37 allow us to find the energy levels of Eq. (2.77), the frequencies of motion inside a barrier, and also decay halfwidths from Eqs. (2.79) and (2.82).

Table III is based on Ref. 37 and it compares the results of numerical calculations of Refs. 28 and 37 for the rates of ionization of a level with $n = 10$ and also the data of Ref. 36 based on the Lanczos theory. We can see that the data of Refs. 28 and 37 agree well but they differ considerably from the earlier results[36] based on the Lanczos theory.

Figure 6 shows the Stark structure of a highly excited lithium atom.[38] It illustrates a set of Stark components corresponding to the projection of the quantum number

TABLE III. Rates Γ of ionization of states corresponding to the $n = 10$ level in an electric field.[37]

n_1n_2m	F, 10^4 V/cm	Γ, sec^{-1}		
		Ref. 36	Ref. 28	Ref. 37
090	4,058	8,236(2)	—	6,889(3)
	4,603	8,015(5)	7(6)	7,090(6)
	5,178	1,425(8)	1,310(9)	1,344(9)
	5,814	7,560(9)	6,707(10)	7,611(10)
900	8,082	1,539(7)	6(6)	5,802(6)
	9,134	8,525(8)	3,170(8)	3,272(8)
	10,81	1,802(10)	6,585(9)	7,675(9)

$|m| = 1$. This set (because of the smallness of the quantum defects of the p states) is very close to the pattern of the Stark splitting in hydrogen. A discrepancy is observed only in the case of the weakest fields when the quantum defect of the p levels is important. We can see clearly the pattern of crossing of the Stark components of various levels. The repulsion between the crossing terms is due to the nonzero value of the quantum defect and on the whole it rises on increase of this defect.[5)] In contrast to nonhydrogen atoms, a nonrelativistic theory of the hydrogen atom admits exact crossing of levels. This is possible because of an additional degeneracy: the crossing levels have not only the parabolic quantum numbers n_1 and m, but can have different values of the additional integral of motion which is the constant of separation of the variables $\alpha_{1,2}$ [Eqs. (2.1) and (2.2)].

On the whole the calculated pattern of the Stark splitting agrees very well with the experimental results.[17,38]

3. ZEEMAN EFFECT

3.1. Atom in a magnetic field

3.1.1. Introductory comments

One of the effects of a magnetic field B on an atom is the well-known Zeeman splitting of atomic levels into separate components corresponding to specific values of the projection of the orbital momentum m of the atom along the direction of the field **B**.

The characteristics of the Zeeman effect which are in particular due to the spin-orbit interaction have been described in detail in a number of textbooks and monographs.[1-3] Therefore we shall consider only the less well-known aspects of the effect observed at high values of the field **B**.

The application of a magnetic field to an atom imposes an additional constraint on the motion of an electron across the field and when this field is increased still further, there is a strong reduction in the transverse motion of an electron and consequent transformation of a three-dimensional potential well of an atom into a one-dimensional well. A considerable change in the energy spectrum of an atom may follow.

We shall initially consider the first-order Zeeman effect in the case of the simplest zero-spin one-electron (hydrogen) atom. The Hamiltonian of a perturbation V due to the interaction of the orbital momentum **l** of an electron with the field **B** is

$$V = -\mu_B \mathbf{l}\mathbf{B}, \tag{3.1}$$

where $\mu_B = e\hbar/2mc$ is the Bohr magneton.

The eigenvalues of the energy can be found (i.e., the perturbation of Eq. (3.1) can be diagonalized) simply by selecting the wave functions corresponding to a specific projection of **l** along the direction of **B**. Usually these functions are spherical wave functions Ψ_{nlm} corresponding to specific values of the total angular momentum $l^2 = l(l+1)$ and on its projection $l_z = \hbar m$. In the case of the hydrogen atom the Zeeman sublevels corresponding to a specific value of m are degenerate in respect of the quantum number l. This special feature of the Coulomb degeneracy is manifested also by the fact that the wave functions of Eq. (3.1) which become diagonalized can be parabolic wave functions $\Psi_{n_1 n_2}$ with the Oz axis along the field **B**. In view of the relationship $n_1 + n_2 + |m| = n - 1$ corresponding to a given value of m these states remain degenerate with the values of n_1 and n_2 corresponding to the constant sum $n_1 + n_2$. Therefore, the Zeeman component of a hydrogen level is characterized not by one but usually by several wave functions. The intensity of the component is governed by the sum over the degenerate states and this sum should no longer depend on the selection of the basis (spherical or parabolic quantization).

In the simplest case of the L_α line (representing the $2 \to 1$ transition) the state with $m = 0$ corresponds to two parabolic functions with $n_1 + n_2 = 1$ and two values of $n_1 - n_2$, which amount to $+1$ and -1 and which represent two different projections of the dipole moment of the atom along the field **B**. Clearly, the sum of the intensities of the transitions from these two states is equal to the intensity of the transition from one "spherical" p state characterized by $l = 1$ and $m = 0$. In general, the transition from the parabolic to the spherical basis is described by the formulas in Eq. (2.10).

3.1.2. Energy spectrum of lower states

We shall consider briefly the evolution of the lower states of the energy spectrum of a hydrogenic atom when the magnetic field B is increased to values comparable with (or exceeding) the intraatomic electric field. This evolution has become important, as already mentioned, in connection with the absorption spectrum of excitons, which are excitations characterized by a very low electron-hole binding energy (because the permittivity of the medium is high and the effective mass of an electron in the medium is small): this energy is comparable with the energy of an electron in a magnetic field of moderate intensity (10–10^2 T). We shall introduce the following parameter as a measure of the field intensity:

$$\gamma = \frac{\mu_B B}{\mathrm{Ry}} \approx 4.26 \cdot 10^{-6}\, B\,(\mathrm{T}), \tag{3.2}$$

where $\mathrm{Ry} \approx 13.6$ eV is the Rydberg constant.

The Hamiltonian of such an atom in a field **B** is[6)]

$$\hat{H} = \frac{1}{2m}\left(\mathbf{p} + \frac{1}{2}\frac{e}{c}[\mathbf{B}\mathbf{r}]\right)^2 - \frac{e^2}{r}. \tag{3.3}$$

In view of the invariance of $\hat{H}$ relative to orientation about the Oz axis, parallel to the field **B** and passing through the nucleus of the atom, the z component of the orbital angular momentum $L_z = -\hbar M$ is conserved. Introducing a cylindrical coordinate system $Oz \| \mathbf{B}$ and bearing in mind that the dependence of the wave function Ψ on the angle of rotation about φ the z axis is trivial, $\Psi \propto e^{iM\varphi}$ we can write the Schrödinger equation in the form

$$\left[\frac{\partial^2}{\partial\rho^2} + \frac{1}{\rho}\frac{\partial}{\partial\rho} + \frac{\partial^2}{\partial z^2} - \frac{M^2}{\rho^2} - 4\gamma^2\rho^2 + \frac{4}{r} + \left(\frac{E}{\mathrm{Ry}} - \gamma M\right)\right]\Psi(\rho, z) = 0. \tag{3.4}$$

The two-dimensional equation (3.4) cannot be solved analytically in its general form because the Coulomb interaction term containing $r = (\rho^2 + z^2)^{1/2}$ prevents separation of the variables. We shall therefore demonstrate the nature of the solution for $\gamma \ll 1$ and $\gamma \gg 1$ and obtain some approximation formulas for the transition range $\gamma \sim 1$.

If $\gamma \ll 1$, allowance for the terms containing γ can be made by using perturbation theory. In the case of the ground

state of the hydrogen atom, this gives[40]

$$E_{100} = -1 + \frac{\gamma^2}{2} - \frac{53}{96}\gamma^4 + \frac{5581}{2304}\gamma^6 - \frac{21577397}{1105920}\gamma^8 + O(\gamma^{10}). \tag{3.5}$$

The expression (3.5) agrees well with the results of numerical calculations up to $\gamma \sim 0.1$ (i.e., up to $B \sim 10^4$ T). Similar results were reported in Ref. 40 for the case when $n = 2$.

If $\gamma \gg 1$, the motion of an electron across the applied magnetic field is governed by the size of its cyclotron orbit $\lambda = (\hbar c/eM)^{1/2}$, whereas along the field it is determined by the Coulomb interaction. The potential of this "longitudinal" Coulomb interaction can be obtained by averaging the total Coulomb potential $e^2(\rho^2 + z^2)^{-1/2}$ over the small parameter of transverse motion. Therefore, bearing in mind that on the average we have $\langle \rho^2 \rangle \sim \lambda \ll \langle z^2 \rangle$, we may assume that the longitudinal motion of an electron occurs in a one-dimensional Coulomb potential.

Successive separation of the transverse and longitudinal types of motion in Eq. (3.4) when $\gamma \gg 1$ can be achieved if the wave function $\Psi(\rho, z)$ is represented as the product of the wave function $\Psi_{NM}(\rho)$ of the transverse motion of an electron in the applied magnetic field and the function $\chi^i_{NM}(z)$ of its longitudinal motion in a one-dimensional "longitudinal" potential.

The transverse motion of an electron in a magnetic field is equivalent, as demonstrated by Eq. (3.4), to the motion of an oscillator whose wave functions are well known[2,7]:

$$\begin{aligned} \Psi_{NM}(\rho) &= \left[\frac{(N-M)!}{2\pi\lambda^2 (N!)^3}\right]^{1/2} (-i)^N \sigma^{M/2} e^{-\sigma/2} L_N^M(\sigma), && M \geqslant 0, \\ &= \left[\frac{(N-M)!}{2\pi\lambda^2 ((N-M)!)^3}\right]^{1/2} (-i)^N \sigma^{-M/2} e^{-\sigma/2} L_{N-M}^{-M}(\sigma), && M < 0, \end{aligned} \tag{3.6}$$

where $N = 0, 1, 2, \ldots$ are integers governing the number of energy (Landau) levels in a magnetic field; $|M| \leqslant N$; $L_N^M(\sigma)$ are the Laguerre polynomials; $\sigma \equiv \rho^2/2\lambda^2$. Consequently, the energy levels of the transverse (oscillator) motion of an electron are

$$E_N = \mathrm{Ry}\,\gamma\left(N + \frac{1}{2}\right). \tag{3.7}$$

The equation for the wavefunctions $\chi^i_{NM}(z)$ of the longitudinal motion is obtained from Eq. (3.4) after averaging over the transverse-motion functions of Eq. (3.6) (Refs. 6 and 7):

$$\left(-\frac{\hbar^2}{2m}\frac{d^2}{dz^2} + V_{NM}(z)\right)\chi^i_{NM} = E^z_{NM_i}\chi^i_{NM}, \tag{3.8}$$

where the energy of the longitudinal motion $E^z_{NM_i}$ should be added to the energy of the transverse motion of Eq. (3.7) and the average potential is given by

$$V_{NM}(z) = \int \Psi^*_{NM}(\rho)\frac{e^2}{(\rho^2+z^2)^{1/2}}\Psi_{NM}(\rho)\,\rho\,d\rho. \tag{3.9}$$

The explicit form of the potential (3.9) is not too complex, so that Eq. (3.8) can be solved analytically. However, it can be approximated satisfactorily by a function of the type[7]

$$V(z) = -\frac{e^2}{a+|z|} + \frac{Ae^2}{(a+|z|)^2}, \tag{3.10}$$

where the size $a \sim \lambda$ and the coefficients A are selected for each NM so as to approximate best the true potential of Eq. (3.9).

If the parameter a is sufficiently small, the potential $V(z)$ is close to a one-dimensional Coulomb potential $e^2/|z|$, as demonstrated by Eq. (3.10). Therefore, by analogy with the three-dimensional Coulomb problem, we shall write down the longitudinal energy $E^z_{NM_{n^*}}$ in the form

$$E^z_{NMn^*} = -\frac{\mathrm{Ry}}{n^{*2}}, \tag{3.11}$$

where the effective "principal quantum number" n^* is obtained from the boundary conditions.

Introducing next a variable $x = (mc^2/\hbar)^{1/2}[(a+z)/n^*]$ and retaining only the first term in the potential of Eq. (3.10), we can reduce Eq. (3.8) to the form

$$\frac{d^2\chi}{dx^2} - \left(\frac{1}{4} - \frac{n^*}{x}\right)\chi = 0, \tag{3.12}$$

the solution of which is in the form of Whittaker functions $W_{n,1/2}(x)$. Bearing in mind also that the potential $V(z)$ does not change as a result of the substitution $z \to -z$, we find that the solutions of Eq. (3.12) should be either even or odd in respect of z. The requirement of continuity of the functions and of their derivatives at $z = 0$ yields the following condition for the odd states:

$$W_{n^*,\,1/2}\left(2\frac{a}{a_0 n^*}\right) = 0, \tag{3.13}$$

whereas in the case of the even states, we obtain

$$\frac{d}{dz}W_{n^*,\,1/2}\left(2\frac{a+z}{a_0 n^*}\right)\Big|_{z=0} = 0. \tag{3.14}$$

The conditions (3.13) and (3.14) give the values of the numbers n^* governing the number of nodes of wave functions and the sequence of the energy levels.

In the limit $\gamma \to \infty$ all the energy levels of the longitudinal motion are hydrogenic, i.e., we have $n^* = 1, 2, \ldots$, with the exception of the ground state the energy of which decreases logarithmically on increase in γ [see Ref. 2, Problem 3 in §112; also Eqs. (3.70) and (3.71) below].

There is a unique relationship between the states in weak and strong magnetic fields. This relationship is found by calculating the number of nodes of a wave function in both limits of weak and strong fields. In fact, an increase in the magnetic field deforms the spherical symmetry of the hydrogen atom to the cylindrical symmetry. Bearing in mind that a free atom is characterized by $n_\rho = n - l - 1$ nodes of the radial wave function, corresponding to n_ρ nodal spheres, and that there are $l - |M|$ nodes of the angular function corresponding to cones with the z axis, and also recalling that in a strong magnetic field we have correspondingly $N - [(|M| + M)/2]$ nodal cylinders ($\rho = \mathrm{const}$) and $2n^*$ (for even states) or $2n^* - 1$ (for odd states) nodal planes intersecting the Oz axis, we find, following Praddaude[41]:

$$\begin{aligned} l - |M| &= 2n^* && \text{— even}, \\ &= 2n^* - 1 && \text{— odd}, \\ n - l - 1 &= N - \frac{|M| + M}{2}, && m = M. \end{aligned} \tag{3.15}$$

For example, the lower even state with $N = 0$, $M = 0$, and

$n^* = 0$ corresponds to $n = 1, l = 0$, and $M = 0$ of the hydrogen atom.

The dependence of the energy E on the parameter γ is described by the formula

$$\frac{\widetilde{E}(\gamma)}{\mathrm{Ry}} = \frac{1}{\mathrm{Ry}}(E_N + E^z_{NMn^*} - \gamma M) = \gamma\left(N - M + \frac{1}{2}\right) - \frac{1}{2n^{*2}}. \quad (3.16)$$

The behavior of the first few levels was calculated by Galindo and Pascual[40] using approximate formulas based on interpolation between the limits $\gamma \to 0$ and $\gamma \to \infty$.

It should be pointed out that the problem of correspondence of the terms and the possibility of their exact crossing has not yet been solved. A magnetic field does not separate the variables (in contrast to an electric field) and the only quantities (apart from the energy) which are conserved are the projection of the momentum and parity. In this case it would seem that the Wigner-Neumann theorem on noncrossing of terms should apply (see 79 in Ref. 2). However, in the case of an atom in a magnetic field there is an additional approximate integral of motion (see Sec. 3.3) which can give rise to exact (or negligibly repelling) crossing of terms. Until the problem is solved finally, we shall follow the identification of the terms given above. This topic is discussed in Ref. 42.

3.2. Adiabatic theory

The results of Sec. 3.1 make possible an interesting generalization to large quantum numbers n corresponding to the motion in a Coulomb well or to rapid motion in a magnetic field ($N \gg 1$). This was done by Zhilich and Monozon[44] and we shall follow their treatment below.

The approach adopted in Ref. 44 is based on the slowness (adiabaticity) of the motion of an electron along a magnetic field (z axis) compared with its motion in a transverse plane. Comparing the classical frequency of motion in a Coulomb field $\omega_n = me^4/\hbar^3 n^3$ with the Larmor frequency $\omega_L = eB/mc$, we obtain the condition

$$\frac{\omega_n}{\omega_L} = \frac{m^2 e^3 c}{\hbar^3 n^3 B} \ll 1. \quad (3.17)$$

The condition (3.17) of slowness of motion of the z coordinate ensures retention of a parametric dependence on z in the wave functions describing the transverse motion, i.e., we can assume that

$$\chi_{Nn}(\rho, z) = R_N(\rho, z)\, W_{Nn}(z). \quad (3.18)$$

Then, Eq. (3.4) yields the following equations for R_N and W_{Nn}:

$$\frac{1}{\rho}\frac{\mathrm{d}}{\mathrm{d}\rho}\rho\frac{\mathrm{d}R_N}{\mathrm{d}\rho} + \left[-\frac{M^2}{\rho^2} + \frac{4}{(\rho^2+z^2)^{1/2}} 4\gamma^2\rho^2 + q_N^2(z)\right] R_N = 0, \quad (3.19)$$

$$\frac{\mathrm{d}^2 W_{Nn}}{\mathrm{d}z^2} + (k^2 - q_N^2(z))\, W_{Nn} = 0, \quad k^2 = 2E - \gamma M, \quad (3.20)$$

where the eigenvalues $q_N^2(z)$ can be found in the $n \gg 1$ case from the Bohr-Sommerfeld quantization conditions

$$\int_{\rho_1(z)}^{\rho_2(z)} \left[q_N^2(z) + \frac{4}{(\rho^2+z^2)^{1/2}} - \frac{M^2}{\rho^2} - 4\gamma^2\rho^2\right]^{1/2} \mathrm{d}\rho = \pi\left(N + \frac{1}{2}\right) \quad (3.21)$$

[$\rho_1(z) < \rho_2(z)$ are the classical turning points representing the roots of the integrand above].

Simple results are obtained from Eq. (3.21) in two limiting cases of $|z| \gg \rho_2(0)$ and $|z| \ll \rho_1(0)$.

If $|z| \gg \rho_2(0)$ then Eq. (3.21) yields an expansion for the eigenvalues

$$q_N^2(z) = -\frac{2}{|z|} + \left(\gamma + \frac{2}{\gamma}\frac{1}{|z|^3}\right)(2N + |m| + 1), \quad (3.22)$$

which determine the form of the effective potential in Eq. (3.20). We can replace this potential by a more general expression of the type

$$\frac{2}{(z^2 + b_N^2)^{1/2}}, \quad b_N^2 = \frac{2}{\gamma}(2N + |m| + 1), \quad (3.23)$$

which is identical with Eq. (3.22) apart from terms of the order of $|z|^{-3}$ if $z \gg b_N$. After this substitution Eq. (3.20) becomes

$$\frac{\mathrm{d}^2 W_{Nn}(z)}{\mathrm{d}z^2} + \left[\frac{2}{(z^2+b_N^2)^{1/2}} - p_{Nn}^2\right] W_{Nn}(z) = 0, \quad (3.24)$$

$$p_{Nn}^2 = -k^2 + \gamma(2N + |m| + 1). \quad (3.25)$$

If $B \to \infty$, Eq. (3.24) clearly reduces to Eq. (3.12) with a one-dimensional Coulomb potential which has the solutions given by Eqs. (3.13) and (3.14). The parameter b_N determines the size of that region along z in which the potential is close to the Coulomb form. Clearly, the size of the Coulomb well decreases more and more as the number N is increased.

Inclusion of corrections of the next order in respect of the adiabaticity parameter (3.17) makes it possible to find the quantum defects $\delta n_{u,g}$ for levels due to deviations of the field from the pure Coulomb form:

$$(p_{Nn}^2) = \frac{1}{(n + \delta n_{u,g})^2} \quad (n = 0, 1, 2 \ldots). \quad (3.26)$$

The quantities $\delta n_{u,g}$ are found for even and odd states on the basis of the solution of Eq. (3.24) [which reduces after the substitution $x^2 = 4p_{Nn}^2(z^2 + b_N^2)$, to an equation in terms of Whittaker functions], subject to the quantization conditions of Eqs. (3.13) and (3.14). The result is[44]

$$\delta n_u = 2b_N, \quad (3.27)$$

$$\delta n_g = -\left(\ln\frac{2b_N}{n}\right)^{-1}. \quad (3.28)$$

Therefore, each doublet level of the hydrogenic atom in a magnetic field splits into two levels corresponding to the quantum defects described by Eqs. (3.27) and (3.28). In the limit $B \to \infty$ the two conditions merge to form a doubly degenerate hydrogenic level of Eq. (3.16).

If $|z| \ll \rho_1(0)$ we can substitute in the quantization condition of Eq. (3.21) an expansion directly in powers of $(z/\rho)^2$. It is easiest to obtain the solution for the case when $M = 0$ [corresponding to $\rho_1(0) = 0$] by assuming that the parameter q_N^2 (proportional to N) is large:

$$q_N^2 = \frac{2}{\rho_2(0)} - \frac{z^2}{\rho_2^3(0)} = \gamma(2N + 1), \quad \rho_2(0) = \frac{2q_N}{\gamma}. \quad (3.29)$$

Solving Eq. (3.29) by the method of successive approximations, we obtain

$$q_N^2(z) = \gamma(2N+1) - \frac{\gamma}{2(2N+1)^{1/2}} + \frac{\gamma^{3/2}}{8(2N+1)^{3/2}} z^2. \quad (3.30)$$

We can see that the effective potential along the z axis coincides in this case with the oscillator potential. The equa-

tion for motion along the z axis becomes

$$\frac{d^2W_{Nn}}{dz^2} - \Omega_N^2 z^2 W_{Nn} + p_{Nn}^2 W_{Nn} = 0, \tag{3.31}$$

where the characteristic frequency of Ω_N electron motion along the z axis is

$$\Omega_N = \frac{\gamma^{3/4}}{2\sqrt{2}\,(2N+1)^{3/4}} \text{ (a.u.)}, \tag{3.32}$$

while

$$p_{Nn}^2 = k^2 - \gamma(2N+1) + \frac{\gamma^{1/2}}{(2N+1)^{1/2}}. \tag{3.33}$$

The spectrum of energy levels E is identical in this case with the oscillator spectrum[44]:

$$E = \frac{\hbar eB}{2mc}(2N+1) - e^2\left[\frac{eB}{4\hbar c\,(2N+1)}\right]^{1/2} + \hbar\left[\frac{e^7B^3}{m^2\hbar^3c^32^6\,(2N+1)^3}\right]^{1/4}\left(n+\frac{1}{2}\right). \tag{3.34}$$

The spectrum of Eq. (3.34) is obtained if the frequency Ω_N is small compared with the Larmor frequency, i.e., when

$$\frac{\Omega_N}{\omega_L} \sim \left(\frac{m^2e^3c}{32\hbar^3BN^3}\right)^{1/4} \ll 1. \tag{3.35}$$

Therefore, the spectrum of bound electrons at a sufficiently high Landau level $N \gg 1$ varies continuously from the oscillator type in the case of low-lying levels to highly excited hydrogenic levels ($n \gg 1$), which become denser at the limit of the series (Fig. 7).

3.3. Level crossing and "latent" symmetry of an atom in a magnetic field

The Hamiltonian $\hat{H}$ of a hydrogen atom in a magnetic field B directed along the z axis is

$$\hat{H} = \frac{\hat{p}^2}{2} - \frac{1}{r} + \frac{1}{2}\omega^2\rho^2 + i\omega\hat{l}_z, \tag{3.36}$$

where l_z is the operator representing the projection of the orbital angular momentum l along the direction of the magnetic field B (Oz axis); $\omega = B/c$ (a.u).

The equations of motion of an atomic electron in a magnetic field do not allow separation of variables in any coordinate system (in contrast to the electric field case) and, consequently, these equations do not contain additional integrals of motion of the type represented by constants of separation of variables. Therefore, when the Zeeman structure of one of the levels overlaps the structure of another level at the crossing points, we cannot expect exact coincidence of the energies (as found in an electric field). Nevertheless, numerical calculations of the Zeeman structure carried out by Zimmerman, Kash, and Kleppner[45] revealed an approximate symmetry of the hydrogen atom in the applied magnetic field. It was manifested by a strong (exponential) fall of the splitting ΔE_n at the points of crossing of the Zeeman sublevels as a function of the principal quantum number n. Figure 8 (taken from Ref. 45) shows the pattern of crossing of the Zeeman sublevels at low and high values of the quantum number n. Clearly, "anticrossing" at low values of n changes to a pattern of almost complete crossing on increase in n. Figure 9 shows how the value of ΔE_n varies on increase in n in the case of crossing of the outer components (continuous line) and of the outer with middle (dashed line) Zeeman components. The dependence on the level number is clearly exponential.

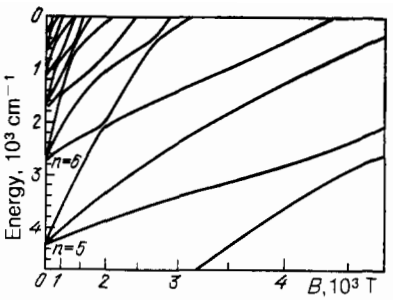

FIG. 8. Crossing of Zeeman energy sublevels E (cm^{-1}) of an atom on increase in a magnetic field B in the case of small values of the principal quantum numbers.[45]

Among the many proposed explanations[45-49] of the approximate symmetry, we shall consider the results of Solov'ev[47] who attributed the observed change in ΔE_n to the presence of an additional integral of motion $\hat{\Lambda}$ for a hydrogen atom in a magnetic field (see also the paper of Herrick[48]). The integral Λ can be obtained, following Ref. 47, using classical equations of motion for the orbital momentum and the Runge-Lenz vector $\mathbf{A} = [\mathbf{p}\times\mathbf{l}] - (\mathbf{r}/r)$ (see Ref. 50) in a magnetic field ($\boldsymbol{\rho} = \mathbf{x} + \mathbf{y}$)

$$\frac{d\mathbf{l}}{dt} = -\omega^2[\mathbf{r}\boldsymbol{\rho}], \quad \frac{d\mathbf{A}}{dt} = -\omega^2\{[\mathbf{p}[\mathbf{r}\boldsymbol{\rho}]] + [\boldsymbol{\rho}[\mathbf{r}\boldsymbol{\rho}]]\}. \tag{3.37}$$

Averaging Eq. (3.37) over the period of motion along an unperturbed trajectory (Kepler ellipse), we obtain a system of equations describing the change in the trajectory under

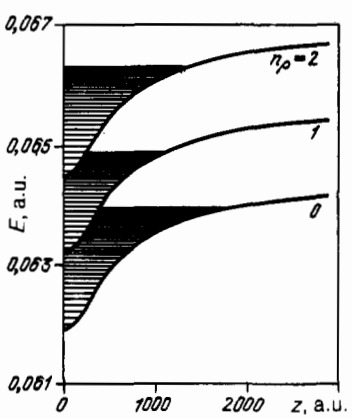

FIG. 7. Energy levels of an excited atom in a strong magnetic field corresponding to a sufficiently high Landau level.

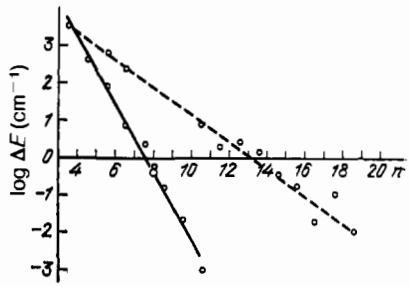

FIG. 9. Variation of the splitting ΔE_n at crossing points of Zeeman sublevels plotted as a function of the principal quantum number n (Ref. 45).

the influence of a magnetic field.

These equations can be used to demonstrate the existence of an integral of motion

$$\Lambda = 4A^2 - 5A_z^2, \tag{3.38}$$

which is conserved together with the energy E and the projection of the orbital angular momentum l_z. Conservation of Λ applies right up to terms of the order of ω^4. Bearing in mind that A^2 varies in the range $0 \leqslant A^2 \leqslant 1$, we can find the range of variation of Λ: $-1 \leqslant \Lambda \leqslant 4$.

The integral of motion Λ gives rise to additional conditions on quantization of angular variables. Let us assume that θ is the angle between the vectors **B** and **A**; then,

$$\Lambda = A^2 (4 - 5 \cos^2 \theta). \tag{3.39}$$

If $\Lambda = 0$, the vector **A** is on a double conical surface described by the condition $\cot \theta_0 = 2$. The conservation of Λ means that all the trajectories of motion can be divided into two classes: trajectories within a double cone (if $0 \leqslant \theta \leqslant \theta_0$; $\pi - \theta_0 \leqslant \theta \leqslant \pi$) or outside it (if $\theta_0 \leqslant \theta \leqslant \pi - \theta$). We can write down the quantization conditions if we introduce a generalized momentum, which is canonically conjugate to the coordinate θ. This is clearly the component of the orbital angular momentum $l_\perp(\theta)$, perpendicular to the plane of the vectors **B** and **A**. Expressing $l_\perp$ in terms of the integrals of motion m, $E(n = -\sqrt{2}E)$, and **A**, we obtain[47]

$$l_\perp(\theta) = [n^2 - U_{\text{eff}}(\theta)]^{1/2}, \quad U_{\text{eff}}(\theta) = \frac{n^2\Lambda}{1 - 5\sin^2\theta} - \frac{m^2}{\sin^2\theta}. \tag{3.40}$$

The effective "angular" potential $U_{\text{eff}}(\theta)$ is plotted in Fig. 2 for the cases $\Lambda < 0$ (a) and $\Lambda > 0$ (b). We can see that the presence of an additional integral of motion results in sharply divided regions of classical motion, defined by the roots of the effective potential $\theta_1, \ldots, \theta_6$. If $\Lambda < 0$ the Bohr-Sommerfeld quantization conditions can be written down separately for the upper and lower parts of a double cone:

$$I_1(\Lambda) = \int_{\theta_1}^{\theta_2} l_\perp(\theta)\, d\theta = \pi\left(k + \frac{1}{2}\right), \tag{3.41}$$

$$I_2(\Lambda) = \int_{\theta_3}^{\theta_4} l_\perp(\theta)\, d\theta = \pi\left(k + \frac{1}{2}\right) \quad (k = 0, 1, 2 \ldots). \tag{3.42}$$

If the potentials in this case are identical, the resultant equations are doubly degenerate. From these states, localized in the upper and lower parts of the cone, we can construct wave functions which are symmetric and antisymmetric relative to the (x, y) plane.

If $\Lambda > 0$, the states are nondegenerate and the quantization condition becomes

$$I_3(\Lambda) = \int_{\theta_3}^{\theta_4} l_\perp(\theta)\, d\theta = \pi\left(k + \frac{1}{2}\right). \tag{3.43}$$

The integrals (3.41)–(3.43) cannot be calculated analytically in general. The maximum value of $I_i(\Lambda)$ is obtained for $\Lambda = 0$ and it determines the total number of states

$$N = \frac{1}{\pi}[I_1(0) + I_2(0) + I_3(0)] = n - m, \tag{3.44}$$

which is identical with the exact quantum number of states with given values of n and m.

In the first (in respect of ω^2) order of perturbation theory the energy is expressed in terms of the period-average value of $\rho^2 = x^2 + y^2$. Calculating this average with the aid of equations for an unperturbed trajectory, we find that[47]

$$E = E_0 + \frac{\omega^2}{2}\bar{\rho}^2 = -\frac{1}{2n^2} + \frac{\omega^2 n^2}{4}(n^2 + m^2 + n^2\Lambda_k). \tag{3.45}$$

The greatest interest lies in the outer Zeeman components which are the first to experience crossing. These sublevels correspond to the lower levels in the effective potentials in Fig. 10 and they can be determined using the parabolic approximation of the potential near its minimum. This gives

$$E = -\frac{1}{2n^2} + \omega^2 n^2 \sqrt{5}\left(k + \frac{1}{2}\right)\{[5(2k+1)^2 + n^2]^{1/2} - \sqrt{5}(2k+1)\} \quad (k = 0, 1, 2 \ldots). \tag{3.46}$$

In going over to quantum mechanics the integral of motion Λ is replaced by the operator Λ which commutes with the Hamiltonian in the subspace of the wave functions with given values of n. This can be demonstrated by expressing the operator $\hat{\rho}^2$, which occurs in the Hamiltonian, in terms of Λ. This relationship makes it possible to construct also wave functions which diagonalize the Hamiltonian of Eq. (3.36) in the subspace of states with a given n. Such construction is possible because of the separation of variables in elliptic-cylindrical coordinates for the hydrogen atom in the case when the independent variables are the operators l_z and the quadratic combinations of the Runge-Lenz vector. We shall not consider the explicit form of these functions, but direct the reader to Refs. 47 and 48, and to the work cited there.

The approximate symmetry of the hydrogen atom associated with the presence of an additional integral of motion Λ, found in Ref. 47, accounts for the relationships deduced from numerical calculations (see Figs. 8 and 9). Indeed, as can be seen from Fig. 10, in the case of states with different values of Λ the splitting at the level quasicrossing points is governed by the penetrability of a classical barrier and if $n \gg 1$, the splitting should be exponentially small. Calculations of the splitting ΔE_n carried out in this way give the result (Ref. 47)[7]:

$$\Delta E_n \approx \exp\left\{-n \ln\left[\frac{1}{2}(\sqrt{5}+2)(\sqrt{5}+1)\right]\right\} \approx \exp(-1.92n). \tag{3.47}$$

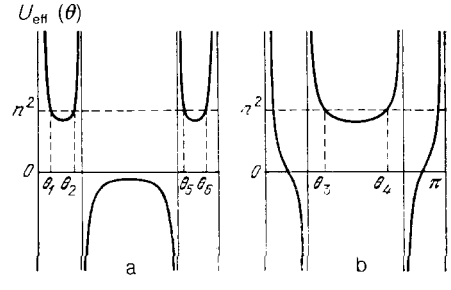

FIG. 10. Effective angular potential $U_{\text{eff}}(\theta)$ for different values of the integral of motion $\Lambda < 0$ (a) and $\Lambda > 0$ (b) based on Ref. 47.

Equation (3.47) indeed demonstrates an exponential fall of the splitting on increase in n, which is close to the calculated data in Figs. 9 and 10.

An interesting approach to a calculation of the quadratic Zeeman effect was developed by Braun[51] and also by Kazantsev *et al.*[52] It is based on the following property of the matrix elements of the perturbation operator $V=x^2+y^2$ expressed in terms of parabolic coordinates (when the axis Oz is parallel to B):

$$V_{n_1n_2}\equiv\frac{n^2}{2}w_{n_1}=\frac{n^2}{2}[3n^2-m^2+1-12(a-n_1)^2],$$

$$V_{n_1n_1-1}\equiv\frac{n^2}{2}p_{n_1}=\frac{n^2}{2}[n_1(n_1+|m|)\times(2a-n_1+1)(2a-n_1+|m|+1)]^{1/2},$$

$$V_{n_1n_1'}=0 \quad \text{when} \quad |n_1-n_1'|\geqslant 2,$$

$$2a\equiv n_1+n_2=n-|m|-1. \tag{3.48}$$

Writing down the wave function with a given value of n as an expansion in terms of parabolic functions $\Psi_{n_1n_2m}$ with the coefficients C_{n_1} and using the property described by the system (3.48), we obtain recurrence relationships for the coefficients C_{n_1}

$$p_{n_1}C_{n_1-1}+(w_{n_1}-\mathscr{E})C_{n_1}+p_{n_1+1}C_{n_1+1}=0, \tag{3.49}$$

where the eigenvalues $\mathscr{E}$ are related to the energy E of an atom by

$$E=-\frac{1}{2n^2}+m\omega_L+\frac{1}{4}\omega_L^2n^2\mathscr{E}+O(\omega_L^4). \tag{3.50}$$

Following Ref. 51, we shall obtain the quasiclassical solution of Eq. (3.49) at high quantum numbers $n_1\gg 1$. We shall do this by representing C_k in the form of the product:

$$C_k=\prod_{s=k_0}^{k}\mu_s=\exp\left(i\sum_{s=k_0}^{k}\Pi_s\right)\approx\exp\left(i\int_{k_0}^{k}\Pi_s\,ds\right), \tag{3.51}$$

where the functions Π_s play the role of the classical momentum in the space of parabolic quantum numbers.

Substituting Eq. (3.51) into Eq. (3.49) and using the condition $n_1\gg 1$, we reduce the recurrence relationships to a quadratic equation of the type

$$p_{n_1}+(w_{n_1}-\mathscr{E})\mu_{n_1}+p_{n_1+1}\mu_{n_1}^2=0, \tag{3.52}$$

the discriminant D_{n_1} of which has the approximate form

$$D_{n_1}\approx(U_{n_1}^+-\mathscr{E})(U_{n_1}^--\mathscr{E}). \tag{3.53}$$

The functions $U_{n_1}^{\pm}$ play a role similar to the potential energy in the Schrödinger equation and, after allowance for Eq. (3.48), these functions are described by

$$U_{n_1}^{\pm}=3n^2-m^2+1-12(a-n_1)^2\pm 8\left\{\left[\left(a+\frac{1}{2}\right)^2-(a-n_1)^2\right]\times\left[\left(a+|m|+\frac{1}{2}\right)^2-(a-n_1)^2\right]\right\}^{1/2}. \tag{3.54}$$

If the energy $\mathscr{E}$ lies within the interval $U_{n_1}^-<\mathscr{E}<U_{n_1}^+$, then $D_{n_1}<0$ and the classical momenta Π_s in Eq. (3.51) become

$$\Pi_k\approx\arccos\frac{\mathscr{E}-w_k}{2p_k+(1/2)}\equiv\arccos B_k. \tag{3.55}$$

The expressions obtained for the "momenta" Π_k can be used also to find the energy $\mathscr{E}$ by applying the Bohr-Sommerfeld quantization rules:

$$\int_{k_1}^{k_1'}\left(s+\frac{1}{2}\right)\frac{dB_s}{ds}\frac{ds}{(1-B_s^2)^{1/2}}=\pi\left(N+\frac{1}{2}\right), \tag{3.56}$$

where $N=0, 1, 2, \ldots$ is an integer.

The nature of the spectrum depends on the potential curves $U_{n_1}^{\pm}$ governed by the projection of the momentum m. For example, if $m=0$, these functions become

$$U_{n_1}^+\approx 5n^2-20(n_1-a)^2, \quad U_{n_1}^-\approx n^2-4(n_1-a)^2, \tag{3.57}$$

i.e., they represent two inverted parabolas with the center at the point $n_1=a$. Classical motion occurs in the range limited by the upper (U^+) and lower (U^-) parabolas. At values of the energy $\mathscr{E}$ less than the maximum of the lower parabola ($U_n^-<\mathscr{E}<\max U_{n_1}^-=n^2$) the motion occurs in two symmetric potential wells separated by a maximum $U_{n_1}^-$. In view of this symmetry the Zeeman sublevels are doubly degenerate. The difference between the energies of these levels $\mathscr{E}_g-\mathscr{E}_u$ is determined by the barrier penetrability and is described, as in the ordinary coordinate space, by a phase integral between the turning points in the subbarrier region. The doublet splitting of the levels disappears for a sufficiently large value of $|m|>n/\sqrt{5}$, corresponding to the region of motion without maxima.

Calculations[51] of the energy $\mathscr{E}_n$ and of the splitting $\mathscr{E}_g-\mathscr{E}_u$ in the case when $m=0$ give the following results. The energy of the lower (doublet) levels deduced from Eq. (3.56) is ($N=0, 1, 2, \ldots$)

$$\mathscr{E}_N=1+4n\sqrt{5}\left(N+\frac{1}{2}\right)-12\left(N+\frac{1}{2}\right)^2+\ldots. \tag{3.58}$$

The corresponding splitting is given by

$$\mathscr{E}_g-\mathscr{E}_u\approx(-1)^n\left(\frac{3-\sqrt{5}}{2}\right)^2(20n^2)^{N+1}\frac{2}{\pi}\left(\frac{e}{2N+1}\right)^{2N+1}\times\exp\left[-\frac{3}{\sqrt{5}}\frac{2N+1}{n}-\frac{9}{4\sqrt{5}}\frac{(2N+1)^2}{n}\right]. \tag{3.59}$$

The formulas (3.58) and (3.59) are strictly valid if $N\ll n$, but a comparison with numerical calculations[51] shows that they are highly accurate even for $N\sim n$.

3.4. Oscillator strengths of transitions

A calculation of the oscillator strengths in a weak magnetic field was carried out by Clark and Taylor[46] by perturbation theory methods. Evolution of the oscillator strengths $f_{nn'}$ of the Zeeman components on increase in the magnetic field B is such that when the Zeeman structures of different levels overlap, there is no significant change in $f_{nn'}$: the components "penetrate" each other freely. As pointed out in Sec. 3.3, this is one of the proofs of the existence of an additional symmetry of an atom in a magnetic field.

The oscillator strengths in ultrahigh magnetic fields have a strong anisotropy due to the existence of a preferred direction $B\|Oz$ (related to the direction of revolution of an electron). A calculation of the oscillator strengths in fields

in the range $B \gg B_0 \gg 10^5$ T based on a general adiabatic theory in Secs. 3.1 and 3.2 above was carried out by Hasegawa and Howard.[7] Following Ref. 7, we shall consider the oscillator strengths for the absorption and emission of circularly polarized light in the xy plane:

$$f_{ij}^{\pm} = \frac{2m}{\hbar^2}\left(E_j - E_i\right)|\langle \Psi_j,\ r_{\pm}\Psi_i\rangle|^2, \quad r_{\pm} = x \pm iy, \tag{3.60}$$

where Ψ_i and Ψ_j are wave functions of the type described by Eq. (3.18), and E_i are the energies of the levels.

It is convenient to introduce generalized momenta $\pi_{\pm}$ and the coordinates X, Y of the center of a cyclotron orbit of an electron:

$$\pi_\alpha = \left(\mathbf{p} + \frac{e}{2c}[\mathbf{Br}]\right)_\alpha, \quad \pi_{\pm} = \frac{1}{2}(\pi_x \pm i\pi_y), \tag{3.61}$$

$$X = x - \frac{\lambda^2}{\hbar}\pi_y, \quad Y = y + \frac{\lambda^2}{\hbar}\pi_x, \tag{3.62}$$

where $\lambda = c\hbar/eB$ is the radius of the cyclotron orbit. The variables π_α, X, and Y obey the commutation relationships

$$[\pi_x,\ \pi_y] = \frac{\hbar}{i\lambda^2}, \quad [X,\ Y] = i\lambda^2, \quad [\pi_\alpha,\ X] = [\pi_\alpha,\ Y] = 0. \tag{3.63}$$

The wave function of the ground state Ψ_0 (usually employed in variational calculations) has the structure

$$\Psi_0 \propto \exp\left(-\frac{x^2+y^2}{4a_\perp^2} - \frac{z^2}{4a_\parallel^2}\right), \tag{3.64}$$

where $a_\perp$ is the transverse size of the orbit approaching the value λ in the limit $B \to \infty$ and $a_\parallel$ is the longitudinal size, which is of the order of the Bohr radius a_0.

Using the operators π_α and the completeness of the system of functions Ψ_i, we readily derive the following rule for the oscillator strengths:

$$\sum_j f_{ij}^{\pm} = \frac{1}{i\hbar}\langle \Psi_i,\ (r_{\mp}\pi_{\pm} - \pi_{\mp}r_{\pm})\,\Psi_i\rangle. \tag{3.65}$$

In the case of the ground state ($i = 0$), using the function (3.64), we obtain

$$\sum_j f_{0\to j}^{\pm} = \frac{1}{2} \pm \frac{a_\perp^2}{2\lambda^2}. \tag{3.66}$$

We can see that in the limit $B \to \infty$ the sum of the oscillator strengths for the left-hand circular polarization (LCP) tends to unity, whereas for the right-hand circular polarization (RCP) it tends to zero.

The matrix elements of the wave functions Φ_{NM} of an electron in a magnetic field are found using the standard properties of the operators $\pi_{\pm}$, X, and Y which are used to describe the relevant coordinate:

$$\pi_{\pm}\Phi_{NM} = \frac{\hbar}{\lambda\sqrt{2}}\binom{N+1}{N}^{1/2} e^{\pm i\theta}\Phi_{N\pm1,\,M\pm1},$$

$$R_{\pm}\Phi_{NM} \propto \Phi_{N,\,M\pm1}. \tag{3.67}$$

The remaining factors of f_{ij} are governed by the overlap integrals of the wave functions F_{NMn} of one-dimensional quasi-Coulomb motion along the z axis. For example, in the case of transitions from the ground state 0 ($N = M = n = 0$) to the first excited states ($N = 1$, $M = 1$, n), we obtain[7]

$$f_{0\to 11n}^{+} = \langle F_{11n},\ F_{000}\rangle^2 - \frac{m\lambda^2}{\hbar^2}\left(\varepsilon_{11n} - \varepsilon_{000}\right)\langle F_{11n},\ F_{000}\rangle \quad \text{(LCP)}, \tag{3.68}$$

$$f_{0\to 0,\,-1,\,n}^{-} = \frac{m\lambda^2}{\hbar^2}\left(\varepsilon_{11n} - \varepsilon_{000}\right)\langle F_{11n},\ F_{000}\rangle \quad \text{(RCP)}, \tag{3.69}$$

where ε_{NM_n} are the energies of longitudinal motion and $\langle F_{11n}, F_{000}\rangle$ are the overlap integrals of the "longitudinal" wave functions.

Calculations of the functions F_{NMn} (and of the associated overlap integrals) are based on a general system for matching the solutions in the range of high and low values of the z coordinate. At high values of z the functions $F_{NMn}(z)$ are identical, according to the results obtained in Sec. 3.1, with the functions in a one-dimensional Coulomb well. At low values of z they can be found by a perturbation method and a characteristic logarithmic singularity is then encountered in integration of the Coulomb potential. Matching the two solutions, we find the energy levels

$$\varepsilon = -\frac{\hbar^2}{2m^2}\frac{1}{a^2n^2} \tag{3.70}$$

and the corresponding form of the wave functions.

The energy of the ground state ($n \to 0$) decreases logarithmically on increase in B:

$$\frac{1}{n} \approx \ln\frac{a^2}{4\lambda^2} + \alpha_{NM} + \ldots, \tag{3.71}$$

The wave functions of the ground state $n = 0$ are concentrated near the origin of the coordinate system so that their overlap integrals are large:

$$\langle F_{i,\,n=0},\ F_{i,\,n=0}\rangle \approx 1 - \frac{4}{\ln(a^2/4\lambda^2)} + \ldots. \tag{3.72}$$

Substitution of Eq. (3.72) in Eq. (3.68) yields the following expression for the oscillator strength involving the ground state

$$f_{0\to 110}^{+} = 1 - \frac{4}{\ln(a^2/4\lambda^2)} + \ldots, \tag{3.73}$$

which is in agreement with the sum rule of Eq. (3.66).

The oscillator strengths for the transitions to states with $n > 1$ can be found similarly. In the case of high values $n \gg 1$ the oscillator strengths $f_{0\to 11n}$ are proportional to a normalization factor n^{-3}. Similarly, we can use the oscillator strength per unit energy interval dn/dE. The wave functions characterized by $n > 0$ have logarithmically small overlap integrals with the function F_{000} concentrated in a region $z \propto \ln^{-1}(a^2/4\lambda^2)$.

Therefore, the corresponding oscillator strengths are small:

$$\frac{dn}{d\varepsilon} f_{0\to 11n}^{+} = 4I^{-3/2}\left(\ln\frac{a^2}{2\lambda^2} - \text{const}\right)^{-1}, \tag{3.74}$$

where

$$I = -\varepsilon_0 = \frac{\hbar^2}{2ma^2}\left(\ln\frac{a^2}{2\lambda^2} - 0.577\right). \tag{3.75}$$

The oscillator strengths for the RCP transitions include an additional small power-law factor.

The general transition scheme, based on Ref. 7, is shown in Fig. 11. The strongest transitions are of type A and these are followed by logarithmically suppressed transitions of type B, and finally by transitions of type C suppressed in a power-law manner.

Detailed calculations of the oscillator strengths for an atom of hydrogen in a magnetic field, including the intermediate range $B \sim B_0$, were carried out by Forster *et al.*[53] Figure

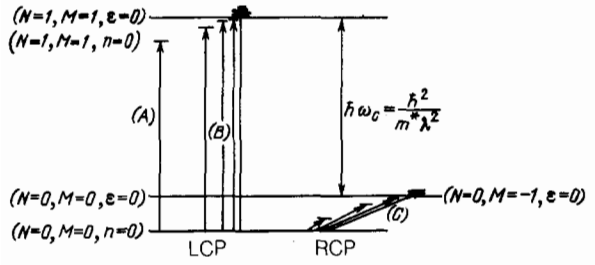

FIG 11. Schematic diagram showing various transitions in an atom subjected to an ultrahigh magnetic field.[7] The quantum numbers N, M, and n of the states are given for right-handed and left-handed circular polarizations (RCP and LCP).

12, based on Ref. 53, shows the behavior of the oscillator strengths $f_{\tau\tau'}$ predicted for various transitions between the lower states of hydrogen. We can see that the transitions allowed in the absence of a magnetic field (of type 1–8) change little the value of $f_{\tau\tau'}$ whereas in the case of other transitions (9–12) the oscillator strengths change by several orders of magnitude.

3.5. Classical trajectories of an atomic electron in a magnetic field

An increase in the intensity of a magnetic field B alters the energy spectrum of an atom from a pure Coulomb (Rydberg) type to a Landau oscillator spectrum with an adjoining one-dimensional quasi-Coulomb spectrum. It is quite difficult to follow in detail such a transition within the quantum theory framework, as found in Secs. 3.1–3.3. However, this can be done on the basis of classical mechanics valid in the case of sufficiently highly excited atomic states. In this case the trajectory of an atomic electron should evolve on increase in B from a Kepler ellipse to Larmor circles. We have shown in Sec. 2.5 that the classical description of the motion of an electron in an electric field F close to the critical value F_c gives good results for probabilistic ionization. We can therefore expect that in the case of a magnetic field a classical description can serve as a satisfactory basis for a future quantum theory.

The classical motion case was investigated in detail by Delos, Knudson, and Noid[54] who solved numerically classical equations of motion of an electron in Coulomb and magnetic fields. We shall follow the treatment given in Ref. 54.

The equations for classical trajectories in cylindrical coordinates $\hat{\rho}$ and $\hat{z}$ (when the Oz axis is parallel to B) can be obtained using a Hamiltonian H containing the Coulomb potential $-e^2(\hat{\rho}^2+\hat{z}^2)^{-1/2}$ the centrifugal potential $L_z^2/2m\hat{\rho}^2$ and a "diamagnetic" term $e^2B^2\hat{\rho}^2/8mc^2$.

The Hamiltonian equations of motion for canonically conjugate coordinates $\hat{\rho}$ and $\hat{z}$ and momenta $\hat{p}_\rho$ and $\hat{p}_z$ can be reduced to a dimensionless form containing just one parameter:

$$L = L_z\left(\frac{e^2B^2}{mc^2}\right)^{1/6} m^{-1/2}e^{-4/3}, \tag{3.76}$$

which is a combination of the parameters of the Coulomb (e^2) and magnetic (proportional to B^2) interactions.

This form of equations is obtained after substitution of variables[8)]

$$\rho=\frac{\hat{\rho}}{\alpha},\quad z=\frac{\hat{z}}{\alpha},\quad p_\rho=\frac{\hat{p}_\rho}{\beta},\quad p_z=\frac{\hat{p}_z}{\beta},\quad t=\frac{\hat{t}}{\gamma}, \tag{3.77}$$

where

$$\alpha=\left(\frac{mc^2}{B^2}\right)^{1/3},\quad \beta=m^{1/2}e^{2/3}\left(\frac{e^2B^2}{mc^2}\right)^{1/6},\quad \gamma=\frac{mc}{eB}. \tag{3.78}$$

In terms of new variables the Hamiltonian $\hat{H}$ contains a single parameter which is the effective z component of the angular momentum L.

The corresponding equations of motion are

$$\begin{aligned}
&\frac{d\rho}{dt}=p_\rho,\quad \frac{dz}{dt}=p_z,\\
&\frac{dp_\rho}{dt}=-\frac{\rho}{(\rho^2+z^2)^{3/2}}-\frac{\rho}{4}+\frac{L^2}{\rho^3},\\
&\frac{dp_z}{dt}=-\frac{z}{(\rho^2+z^2)^{3/2}}.
\end{aligned} \tag{3.79}$$

The trajectories of an electron in terms of the variables ρ, z, p_ρ, and p_z are still complex. However, we can obtain a full picture of these trajectories by considering a section obtained by cutting with the $z=0$ plane (Poincaré section[55]). In fact, it is clear from the system of equations (3.79) that d^2z/dt^2 and z always have opposite signs. Therefore, this system must be intersected by the $z=0$ plane throughout the whole duration of motion $-\infty<t<+\infty$. Numerical calculations of trajectories reported in Ref. 54 were carried out as follows: it was assumed that $z=0$ and for given H and L selection was made of twenty random values of the variables ρ and p_ρ; p_z was deduced from the Hamiltonian and this was followed by solution of the equations of motion giv-

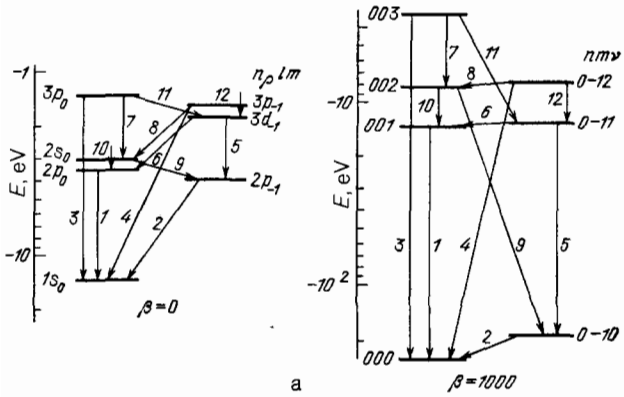

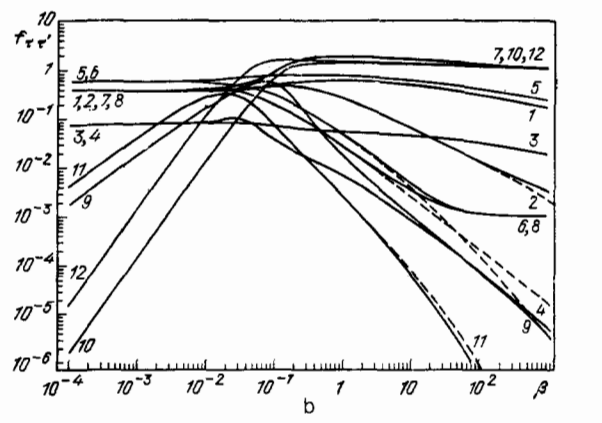

FIG. 12. Changes in the oscillator strengths $f_{\tau\tau'}$ of transitions between the lowest states of the hydrogen atom on increase in the magnetic field (parameter $\beta=B/B_0$).[53] The dashed curves correspond to the approximation of an infinite proton mass. The scheme of transitions corresponding to $\beta=0$ and $\beta=10^3$ is shown in Fig. 12a.

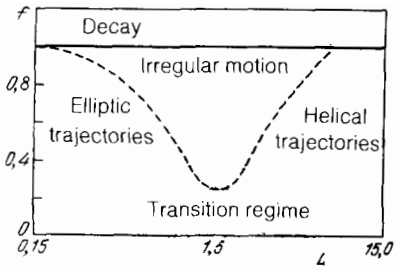

FIG. 13. Schematic representations of the regions of electron motion in the plane of dimensionless energies $f=[E-E_{min}(L)][E_s(L)-E_{min}(L)]^{-1}$ and of the angular momentum L (Ref. 54). Ranges of existence of various types of motion are indicated.

en by the system (3.79).

We shall first consider the general aspects of motion. An electron moves in an effective potential

$$V(\rho, z) = -(\rho^2+z^2)^{-1/2}+\frac{L^2}{2\rho^2}+\frac{\rho^2}{8}, \qquad (3.80)$$

which has two characteristic values: a minimum at $z_0 = 0$ at the point ρ_0:

$$\frac{\rho_0^4}{4}+\rho_0-L^2=0, \quad V(\rho_0)=E_{min}(L), \qquad (3.81)$$

as well as an energy E_s for the detachment of an electron from a nucleus in the limit $z\to\infty$:

$$\rho_s=(2L)^{1/2}, \quad V(\rho_s, \infty)=\frac{L}{2}=E_s(L). \qquad (3.82)$$

It is convenient to describe the motion of an electron of energy E by introducing a dimensionless energy

$$f = (E - E_{min}(L))(E_s - E_{min}(L))^{-1}, \qquad (3.83)$$

which vanishes at $E = E_{min}$ and becomes unity at $E = E_s$.

Figure 13 shows schematically the regions characterized by different types of motion in the (f, L) plane. Elliptic motion at low values of L (corresponding to weak fields B) changes to helical motion at high values of L (strong fields B). Phase trajectories (paths) in the $z = 0$ plane are plotted in Fig. 14 for several values of f and L.

Following Ref. 54, we shall describe the motion of an electron in each of the regions in the (f, L) plane.

a) *Elliptic trajectories* correspond to the usual motion along Kepler ellipses. Among these we can identify ellipses elongated along the positive or negative axes (known as "librators"). The motion along "librators" occurs[54] if $E \gtrsim -1/10L^2$, i.e., in a narrow region of the (f, L) plane in Fig. 13. These trajectories apparently play an important role in the transition to unstable motion (see below). The bulk of the trajectories (known as "rotators") correspond to motion along ellipses close to the (x, y) plane.

b) *Helical trajectories* occur in a strong magnetic field and correspond, as in the quantum theory in Sec. 3.2, to a sharp division of periods of motion along (parallel to the Oz axis) and across the applied magnetic field. As in Sec. 3.2, we can adopt adiabatic separation of the motion in the Hamilton-Jacobi equation retaining a parametric dependence of the potential $V(\rho, z)$ on z.

The nature of the energy spectrum obtained using semiclassical quantization conditions is of the kind shown in Fig. 7.

c) *Irregular motion* occurs when the interactions of an electron with the Coulomb and magnetic fields are comparable, and it is manifested by the fact that a trajectory fills continuously the phase (p_ρ, ρ)-space (Figs. 14c–14i). The

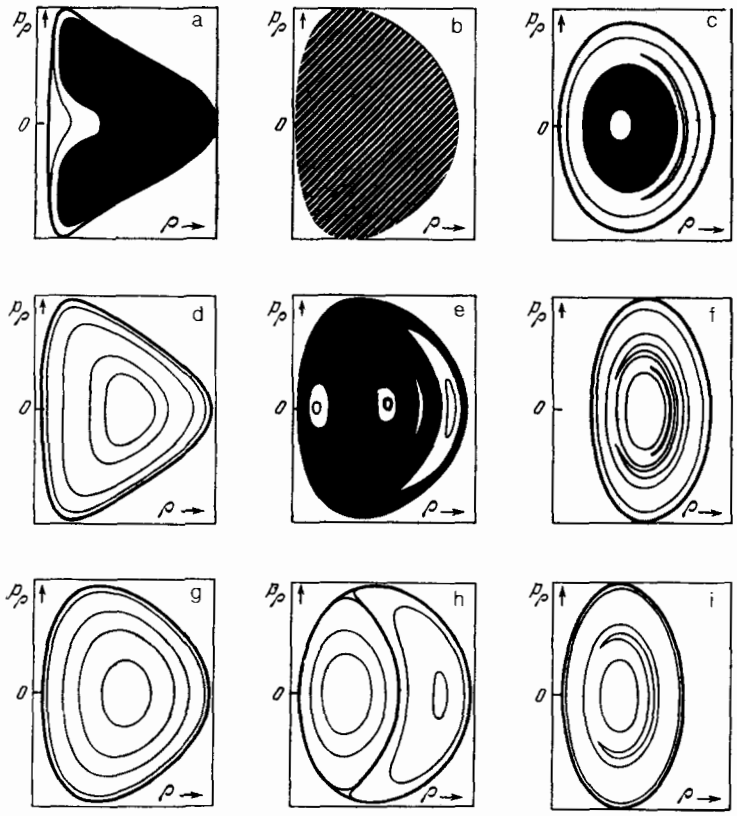

FIG. 14. Phase trajectories $(p\rho, \rho)$ of an electron in the $z = 0$ plane obtained for different values of f and L (Ref. 54). The columns from left to right correspond to $L = 0.50$, 1.51, and 5.03, respectively, whereas the rows counting upwards from the bottom correspond to $f = 0.1$, 0.4, and 0.8, respectively. The black regions represent stochastic trajectories.

mechanism of appearance of stochastic motion in this case is not yet fully understood, but it is obviously related to resonances of two existing types of periodic motion: along a Kepler ellipse and along a Larmor circle.

d) *Transition motion* is observed also for comparable intensities of the interactions, but at lower energies f and it represents stable motion. If $L \sim 1.5$, this motion is however different from ellipses and circles. At low energies f the motion occurs near a minimum of the effective potential and can be investigated by a quadratic expansion of this potential $[U(\rho) \propto (\rho - \rho_0)^2]$. Consequently, the potential becomes oscillatory in respect of the variables ρ and z; the trajectory is then close to that of a two-dimensional oscillator.

We shall conclude our account of classical calculations by estimating the regions of appearance of transition effects in the case of a hydrogen atom in a magnetic field. If we express the parameter L in terms of the initial parameters B (in teslas) and L_z (in units of $\hbar$), we obtain $L_z B^{1/3} = 61.6L$. In a field of $B \sim 10$ T for an intermediate value of $L \sim 1.5$, we find that $L_z \sim 40\hbar$. These values of L_z can however decrease to a few units in the case of hydrogenic excitons in a medium with a permittivity ~ 10 and an effective electron mass $0.1m_e$.

3.6. Stochastization of electron motion in Coulomb and magnetic fields

Following Robnik,[49] we shall consider in greater detail the appearance of unstable motion of an electron in Coulomb and magnetic fields. Such motion is due to a resonance interaction of modes representing the motion in these fields and the range of its manifestation becomes narrower when one of the interactions becomes stronger. Therefore, there is a definite range of parameters (representing projections of the orbital angular momenum L, the energy E, and the field B/B_0) in which electron trajectories cover uniformly (but randomly) the range of allowed motion in the phase space (Fig. 14).

The transition to random motion had been investigated both by Robnik[49] and by Delos, Knudson, and Noid[54] and in both cases this was done numerically using classical mechanics. Figure 15 shows the behavior of the points of intersection of electron trajectories by the $z = 0$ plane (Poincaré section; see Ref. 55) for various values of the energy E and the parameters $L = 1$ and $\gamma = B/B_0 = 1$. The motion on a trajectory represents mapping of points on the phase plane (p_ρ, ρ) representing periodic intersection of the trajectory by the $z = 0$ plane. It is of interest to consider fixed points and invariant curves which are not affected by successive mapping. The minimum and maximum values of the energy in Fig. 15 are $E_{min} = -0.394...$ and $E_{max} = 0.5$. We can see that when the energy is low (Fig. 15a) the phase space consists of invariant curves corresponding to periodic motion of an electron along the trajectories. The existence of such curves is proof of the existence of an additional (third) integral of motion $I_3(p, q)$ which defines an invariant surface $I_3(p, q) = \text{const}$ and the points of intersection of this surface with the plane $(\rho, p_\rho, z = 0)$ form invariant curves. At the centers of these curves there is a fixed imaging point corresponding to totally periodic motion.

An increase in the energy E (Fig. 15c) results in bifurcation that gives rise to a second fixed point surrounded by a family of closed curves. When the energy is $E = -0.04$ (Fig. 15d) the structure of the trajectories changes drastically: curves with multiple intersections appear and in the corners of such intersections there is an accumulation of points (with a nonzero measure), so that these curves are no longer the usual lines and on further increase in E (Fig. 15e) these curves broaden into a uniformly filled layer. A further increase in E produces a more or less uniform broadening of the layer (alternating with regions of regular motion) and subsequently gives rise to uniform filling of the whole region of allowed motion in the phase space. The value $E = E_c = -0.04$ at which there is an abrupt change in the nature of the trajectories is called the critical energy. Therefore, if $E < E_c$, the motion occurs mainly along invariant curves corresponding to different values of the conserved invariant $I_3(p,q)$. If $E > E_c$, this invariant is lost and the motion inside the allowed region is uncorrelated (chaotic). A detailed mechanism of stochastization (of the type representing overlap of the resonances[55]) has not yet been finally identified and, moreover, the explicit form of the integral $I_3(p, q)$ is not known. Therefore, it is not clear whether this integral corresponds to the approximate classical integral Λ found in Refs. 47 and 48 (see Sec. 3.3).

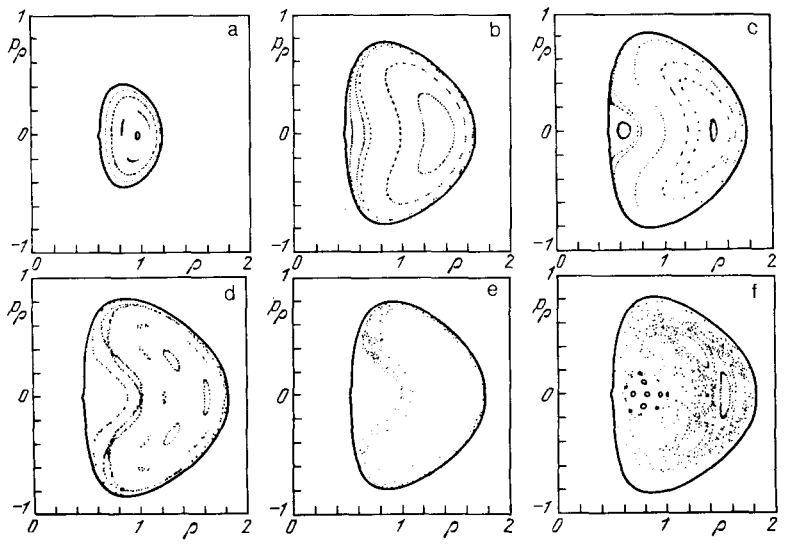

FIG. 15. Behavior of phase trajectories of an electron plotted for the parameters $L = 1$ and $\gamma = B/B_0 = 1$ and different energies E (a.u.): a) -0.3; b) -0.1; c) -0.05; d) -0.04; e) -0.04; f) 0.

Nevertheless, numerical calculations[49] make it possible to determine the unstable region. We note that the Hamiltonian H and, consequently, the parameters E_{min} and E_s depend only on the combination γL^3 (after change of all variables to the dimensionless form with the aid of L), so that calculations carried out for $L = 1$ can be used to obtain results for any value of L. In Ref. 49 the ratio f of Eq. (3.83) is calculated near the critical fields $E = E_c$. The minimum value of f_{min} is 0.22 for $\gamma L^3 \approx 2.7$. Above the curve $f(E_c, \gamma L^3)$ we have irregular stochastic motion of an electron, whereas below it the motion is regular and quasiperiodic (see Fig. 13). It follows from the scaling parameter γL^3 that the magnetic fields in which stochasticity appears decrease rapidly (proportionally to L^{-3}) on increase in L. A reduction or an increase in the parameter γL^3 results in predominance of either the Coulomb or the magnetic interaction. This narrows down the range of stochastic behavior. The relationship between this classical description of the motion of an electron and numerical quantum calculations is in many respects still unclear. This applies both to the region of regular classical motion and (even more so) the region of stochastic motion. In any case, we are dealing here with the case of quantization of motion with unseparable variables, which is of fundamental and practical importance.

3.7. Numerical calculations of spectra of an atom in a magnetic field

Large numbers of numerical calculations[41,43,45,47,53,56–58] of the spectra of the hydrogen atom in a strong magnetic field have been carried out either by perturbation theory methods or on the basis of asymptotic expansions in terms of the field B. Some results of the calculation and interpolation formulas for lower excited states based on these calculations are given Sec. 3.1.

Sufficiently convenient universal data for arbitrary atomic levels in any field B are not yet available, although the results of calculations carried out for a number of states in various ranges of variation B are in good mutual agreement.[9)]

It is appropriate to mention here a simple circumstance[60] associated with the behavior of atomic terms in the region of transition from ultrahigh magnetic fields B to low fields. A direct comparison of calculations carried out for low fields in a spherical basis subject to a diamagnetic perturbation with calculations for high magnetic fields gives results very similar to more rigorous numerical calculations.

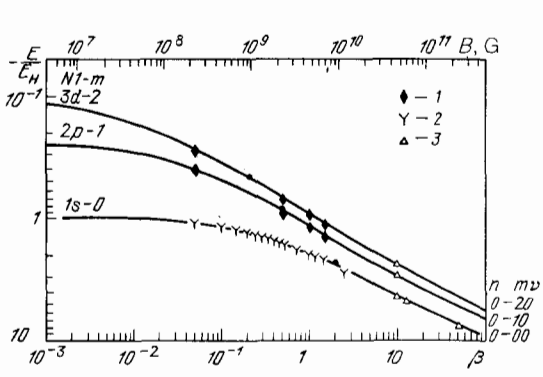

FIG. 16. Comparison of the behavior of atomic terms found by direct combination of the results for $\beta \ll 1$ and $\beta \gg 1$ with the results of more accurate numerical calculations[60]: 1) Ref. 41; 2) Ref. 43; 3) Ref. 42. The points are the places where the terms were combined.

A comparison of the results obtained by direct joining of the results corresponding to the two limiting cases of low and high fields B with those obtained by more rigorous calculations is made in Fig. 16 (Refs. 41–43). We can clearly see that the curves agree throughout the full range of B. This demonstrates that modification of the atomic basis of the states from Kepler orbits to cyclotron revolution occurs in a narrow range of B. This is also supported by the results of a classical calculation of electron trajectories (see Sec. 3.5) demonstrating the feasibility of simultaneous coexistence of Kepler and cyclotron orbits. Clear ideas on the transformation of wave functions of the energy states can be provided by the results of numerical calculations of Rosner *et al.*[61]

3.8. Simultaneous effects of F and B fields on an atom

3.8.1. First-order effects

Simultaneous action of electric and magnetic fields on an atom is encountered in many practical applications. In particular, such simultaneous action occurs when an atom is situated in a magnetized plasma where an electric field F is created by the surrounding charged particles[62,63]

Crossed **F–B** fields also appear when atoms move across a magnetic field because in the system of coordinates linked to an atom there is an electric (Lorentz) field $\mathbf{F}_L = [\mathbf{v} \times \mathbf{B}]/c$. This gives rise to a dependence of the energy levels of the atom on its velocity, which is of considerable interest for an atom in a plasma and for excitons in a solid. The dependence of the energy levels of an exciton in a strong magnetic field on its momentum across the magnetic field was first investigated by Gor'kov and Dzyaloshinskii[64]

Frequently the appearance of an effective magnetic field is due to a change to a rotating system of coordinates. Such a change is convenient in many physical problems, including magnetic resonance,[65] an atom in a rotating electric field,[66,67] or in a field of circularly polarized light,[68] an atom in the field of a moving charge,[69,70] etc. We have to distinguish here the problems where there is a true interaction with a magnetic field and an effective interaction due to rotation of the coordinate system. In the former case we always have a diamagnetic perturbation, whereas in the latter case there are only quadratic corrections to the Zeeman effect. However, this distinction is unimportant in the first order of perturbation theory.

The problem of the behavior of an atom in **F** and **B** fields was considered a long time ago using classical mechanics.[71]

We shall consider the period-average characteristics of motion of an electron in fields F and B. We shall do this by using an additional integral of motion in a Coulomb field (Runge-Lenz vector) related to the period-average value of the coordinate $\langle \mathbf{r} \rangle$:

$$\mathbf{A} = -\frac{2}{3}\frac{e^2}{a}\langle \mathbf{r} \rangle \qquad \left(a = \frac{e^2}{2|E|}\right). \tag{3.84}$$

In the case of period-average values of the orbital angular momentum $\mathbf{M}$ of an atom and of the vector $\mathbf{A}$ in a static electric field $\mathbf{F}$, we obtain the following equations[72]

$$\dot{\mathbf{M}} = \frac{3}{2}\frac{a}{e^2}[\mathbf{FA}], \quad \dot{\mathbf{A}} = \frac{3}{2m}[\mathbf{FM}]. \tag{3.85}$$

In a uniform magnetic field a classical particle rotates (revolves) at an angular velocity $\Omega_B = -eB/2mc$, which cor-

responds to the equations

$$\dot{\mathbf{M}} = [\Omega \mathbf{M}], \quad \dot{\mathbf{A}} = [\Omega \mathbf{A}]. \tag{3.86}$$

If a particle is subjected simultaneously to both **F** and **B** fields, the corresponding equations of motion for **M** and **A** are obtained by adding Eqs. (3.85) and (3.86). Introducing new vectors representing the angular momentum

$$\mathbf{J}_{1,2} = \frac{1}{2}\left[\mathbf{M} \pm \left(\frac{m}{a}\right)^{1/2} \mathbf{A}\right] \tag{3.87}$$

and the frequency

$$\omega_{1,2} = \Omega \pm \frac{3}{2} F \left(\frac{a}{m}\right)^{1/2}, \tag{3.88}$$

we can rewrite the equations of motion in the form[71,72]

$$\dot{\mathbf{J}}_1 = [\omega_1 \mathbf{J}_1], \quad \dot{\mathbf{J}}_2 = [\omega_2 \mathbf{J}_2]. \tag{3.89}$$

It is clear from Eq. (3.89) that the new angular momenta $\mathbf{J}_1$ and $\mathbf{J}_2$ precess at frequencies ω_1 and ω_2 independently of one another. The correction V_1 to the energy of a particle in fields **F** and **B** expressed in terms of the variables **J** and ω is

$$V_1 = \mathbf{J}_1 \omega_1 + \mathbf{J}_2 \omega_2. \tag{3.90}$$

Therefore, the change in the energy is determined by the projections of the vectors $\mathbf{J}_{1,2}$ along the directions $\omega_{1,2}$.

The form adopted in Eq. (3.90) provides a simple opportunity for the generalization of the results to the quantum case. This can be done by independent quantization of the projections of the momenta $\mathbf{J}_1$ and $\mathbf{J}_2$ identified by quantum numbers n' and n'':

$$V_1 = n'\hbar \mid \omega_1 \mid + n''\hbar \mid \omega_2 \mid. \tag{3.91}$$

The numbers n' and n'' assume, in accordance with the definitions of $\mathbf{J}_1$ and $\mathbf{J}_2$, half-integral values: $-(n-1)/2 \leqslant n'$, $n'' \leqslant (n-1)/2$.

Consistent quantum-mechanical generalization of the classical results was provided by Demkov, Monozon, and Ostrovskiĭ.[73] The "correct" wave functions $\Psi_{nn'n''}$ corresponding to the diagonalized Hamiltonian of Eq. (3.90) can be obtained from parabolic wave functions $\Psi_{ni_1i_2}$ corresponding to specific projections i_1 and i_2 of the vectors $\mathbf{J}_1$ and $\mathbf{J}_2$ along the electric field, and this can be done by rotation through angles β_1 and β_2 between the vectors $\omega_{1,2}$ and the direction of the field **F** (Ref. 73):

$$\Psi_{nn'n''} = \sum_{i_1, i_2} D^{(n-1)/2}_{n'i_1}(0, \beta_1, 0)\, D^{(n-1)/2}_{n''i_2}(0, \beta_2, 0)\, \Psi_{ni_1i_2}. \tag{3.92}$$

Here, $D^{(j)}_{k,l}(0,\beta,0)$ are the Wigner rotation matrices[73] describing rotation by angles $\beta_{1,2}$ given by the relationships (in the **F**⊥**B** case)

$$\operatorname{tg} \beta_2 = \Omega \left(\frac{3}{2\hbar} n e a_0 F\right)^{-1}, \quad \beta_1 + \beta_2 = \pi. \tag{3.93}$$

If $B = 0$ the angles $\beta_1 = \pi$ and $\beta_2 = 0$ and the functions $\Psi_{nn'n''}$ are identical with the usual parabolic functions $\Psi_{ni_1i_2}$ corresponding to the Stark effect. If $F = 0$, then the angles $\beta_{1,2} = \pi/2$ and the functions $\Psi_{nn'n''}$ transform into parabolic functions oriented along the magnetic field B. The relationship between them and spherical functions is considered in Sec. 3.1.1.

It is of special interest to consider the case of mutually perpendicular fields **F** and **B**, when the change in the energy is

$$V_1 = \hbar (n' + n'') \mid \omega_{1,2} \mid$$
$$= \hbar (n' + n'') \left[\left(\frac{3}{2} n \frac{a_0}{\hbar e}\right)^2 F^2 + \Omega_B^2\right]^{1/2}. \tag{3.94}$$

Here, we are dealing with an additional degeneracy of the levels due to the fact that the energy V_1 depends only on the sum of the quantum numbers $n' + n''$ and not on each of the numbers n' and n'' separately.

3.8.2. Second-order corrections

Calculations in the second order of perturbation theory on a hydrogen atom subjected to **F**–**B** fields are much more difficult. They were considered by Solov'ev.[74] One has to allow here for the second-order corrections due to the perturbation V_1 of Eq. (3.90) and for the first order of the diamagnetic perturbation $V_2 = [\mathbf{B} \times \mathbf{r}]^2/8c^2$. The magnetic interaction included in V_1 makes no contribution because the resultant matrix elements of this interaction, which are off-diagonal in respect of n, vanish. Consequently, the effective operator $\hat{\Lambda}$ allowing for the second-order corrections is[74]

$$\hat{\Lambda} = \hat{V}_2 - F^2 z G_n z \equiv \hat{V}_2 + \hat{W} F^2, \tag{3.95}$$

where G_n is the Coulomb Green's function including summation over all intermediate states of the investigated atom.

The operator $\hat{V}_2$ associated with the diamagnetic interaction is expressed above (Sec. 3.3; see also Ref. 47) in terms of the angular momentum operator L and the Runge-Lenz vector **A**:

$$\hat{V}_2 = \frac{n^2 B^2}{16c^2}(n^2 + 3 + L_B^2 + 4A^2 - 5A_B^2), \tag{3.96}$$

where L_B and A_B are the projections of these operators along the magnetic field direction.

A similar expression in the space of states with a given value of n can be obtained also in the case of $\hat{W}$ (when the Oz axis is parallel to the field **F**):

$$\hat{W} = \frac{n^4}{16}(5n^2 + 31 + 24L^2 - 21L_z^2 + 9A_z^2). \tag{3.97}$$

Expressing next the operators **L** and **A** in terms of new angular momentum operators $\mathbf{J}_1$ and **J**, and using the wave functions $\Psi_{nn'n''}$ of Eq. (3.92), which correspond to specific projections of these operators, we obtain the second-order correction to the energy[74]:

$$E^{(2)} = -\frac{n^4 F^2}{16}[17n^2 + 19 - 12(n'^2 + n'n'' \cos\gamma + n''^2)]$$
$$+ \frac{n^2 B^2}{48c^2}[7n^2 + 5 + 4n'n'' \sin\gamma_1 \sin\gamma_2$$
$$+ (n^2 - 1)(\cos^2\gamma_1 + \cos^2\gamma_2)$$
$$- 12(n'^2 \cos^2\gamma_1 - n'n'' \cos\gamma_1 \cos\gamma_2 + n''^2 \cos^2\gamma_2)], \tag{3.98}$$

where γ_1 and γ_2 are the angles between the vector **B** and the vectors ω_1 and ω_2; $\gamma = \gamma_1 + \gamma_2$.

The results are valid only on condition that the degeneracy of the levels is lifted in the first order of perturbation theory. This condition breaks down in the case of mutually perpendicular fields F and B when the frequencies ω_1 and ω_2

are equal: $\omega_1 = \omega_2 = \omega$, and when the first-order correction depends only on the sum of the quantum numbers $n' + n''$. Therefore, Eq. (3.98) gives the correct result if the difference between ω_1 and ω_2 exceeds the correction $E^{(2)}$. The case $\mathbf{F} \perp \mathbf{B}$ cannot be considered analytically in the second order of perturbation theory. The general calculation procedure in this case involves numerical diagonalization of bilinear combinations of the angular momenta $\mathbf{J}_1$ and $\mathbf{J}_2$ in the subspace of quantum numbers n' and n'', and it is given in Ref. 74.

The behavior of the ground state of the hydrogen atom subjected simultaneously to electric and magnetic fields was considered by Turbiner[75] by the methods of perturbation theory. The expansion for the energy can be represented conveniently in the form

$$E = E_{SZ} + E^{(\parallel,\perp)}, \tag{3.99}$$

where E_{SZ} is the sum of the energies of the fields F and B taken separately:

$$E_{SZ} = -1 - \frac{9}{2} F^2 + \frac{B^2}{2} - \frac{3555}{32} F^4 - \frac{53}{96} B^4 + \ldots, \tag{3.100}$$

and $E^{\parallel,\perp}$ contains the hitherto unknown cross terms for mutually parallel ($E^{\parallel}$) and perpendicular ($E^{\perp}$) directions of the fields F and B:

$$E^{\parallel} = \frac{159}{16} F^2B^2 - \frac{1\,742\,009}{26\,880} F^2B^4 + \ldots, \tag{3.101}$$

$$E^{\perp} = \frac{93}{4} F^2B^2 - \frac{22\,770\,991}{107\,520} F^2B^4 + \ldots . \tag{3.102}$$

The results represented by Eqs. (3.99)–(3.102) allow us to understand qualitatively the characteristics of the behavior of an atom in fields F and B. Indeed, if we assume that the electric field F is constant, we can find the magnetic susceptibility of the investigated atom[75]:

$$\chi^{\parallel} = -1 - \frac{159}{8} F^2 + \frac{53}{24} B^2 + \frac{1\,742\,009}{6\,720} F^2B^2 + \ldots,$$
$$\chi^{\perp} = -1 - \frac{731}{24} F^2 + \frac{53}{24} B^2 + \frac{15\,308\,863}{30\,240} F^2B^2 + \ldots . \tag{3.103}$$

We can see that the sign of the term with the electric field (proportional to F^2) is opposite to the sign of the usual "diamagnetic" term (proportional to B^2). Therefore, the presence of the electric field increases the magnetic susceptibility of the atom. It should be pointed out that this effect is stronger in the case when $\mathbf{F} \perp \mathbf{B}$.

On the other hand, if we fix the value of B, we can find the influence of this field on the polarizability of the atom in the field F (Ref. 75):

$$\alpha^{\parallel} = 9 + \frac{3\,555}{8} F^2 - \frac{159}{8} B^2 + \frac{1\,742\,009}{13\,440} B^4 + \ldots,$$
$$\alpha^{\perp} = 9 + \frac{3\,555}{8} F^2 - \frac{731}{24} B^2 + \frac{15\,308\,863}{60\,480} B^4 + \ldots . \tag{3.104}$$

We can see that the magnetic field reduces effectively the polarizability of the investigated atom.

3.8.3. Atom in electric and strong magnetic fields

The limits of a strong magnetic field ($B \gg B_0$) and a weak magnetic field ($F \ll B$) were considered in Ref. 74 in the specific case, mentioned above, of energy levels of an exciton moving across a magnetic field.

A detailed description of the structure of such spectra is outside the scope of the present review. We shall consider only an interesting feature of the spectrum of an atom of hydrogen in crossed F and B fields, which was investigated by Burkova *et al.*[76]

The characteristics of motion of a free charge in F and B fields are related, as is known, to the drift of the charge at a velocity

$$\mathbf{v}_d = c \frac{[\mathbf{FB}]}{B^2}, \tag{3.105}$$

which is the same for an ion (of mass m_i) and for an electron (of mass m_e).

The drift of an electron may give rise to new bound states in an atom localized at a certain distance y_0 equal to the drift displacement during an effective cyclotron oscillation period[76]:

$$y_0 = v_d \left[\frac{eB}{(m_i + m_e)c}\right]^{-1} = \frac{Mc^2F}{eB^2} \qquad (M \equiv m_i + m_e). \tag{3.106}$$

The spectrum of an atomic electron can be obtained conveniently in this case by transforming the wave function to a system of coordinates linked to the drift motion[64]:

$$\Psi = \Phi \exp \frac{i\gamma Mc\,[\mathbf{BF}]\,\mathbf{r}}{2\hbar B^2}, \tag{3.107}$$

where $\gamma = (m_i - m_e)/M$.

If the z axis is directed along the field $\mathbf{B}$ and the y axis along the field $\mathbf{F}$, and if the origin of the coordinate system is shifted along the y axis by an amount y_0, the Schrödinger equation becomes[76]

$$\left\{-\frac{\hbar^2}{2\mu}\Delta_\rho - \frac{\hbar^2}{2\mu}\frac{\partial^2}{\partial z^2} + \frac{ie\hbar\gamma}{2mc}[\boldsymbol{\rho}\boldsymbol{\nabla}_\rho]\,\mathbf{B} + \frac{e^2}{8\mu c^2}B^2\rho^2 - e\left[x^2 + (y + y_0)^2 + z^2\right]^{-1/2} - Mc^2F^2(2B^2)^{-1}\right\}\Phi = E\Phi, \tag{3.108}$$

where $\mu = m_e m_i/M$ is the reduced mass.

We shall consider the effective potential energy U along the y axis:

$$U = \frac{e^2B^2}{8\mu c^2} y^2 - \frac{e^2}{|y + y_0|} - \frac{Mc^2F^2}{2B^2}. \tag{3.109}$$

We can see that the potential U can have two wells: one Coulomb well at $y \approx y_0$ and the second at $y = 0$. Such a structure of the potential is realized for a sufficiently large value of the following parameter

$$\left(\frac{M}{\mu}\right)^{1/2} \frac{\hbar c}{e^2} \frac{F}{B} \left(\frac{B}{B_0}\right)^2 > 1, \tag{3.110}$$

when the bottom of the well at $y = 0$ is higher than the Coulomb binding energy $me^4/\hbar^2$.

The energy spectrum can be calculated subject to the condition (3.110) if, as in Sec. 3.1, we separate the variables of the longitudinal (along the z axis) and transverse motion, and if we reduce the Schrödinger equation of Eq. (3.108) to the one-dimensional form with an effective potential $u(x, y, z)$ obtained by averaging the initial potential over the transverse coordinates ρ:

$$u = -e^2 \int \frac{\Phi(\rho)\,d\rho}{[x^2 + (y + y_0)^2 + z^2]^{1/2}}, \tag{3.111}$$

where $\Phi(\rho)$ is the wave function of the transverse motion with a characteristic scale length a_B (see Secs. 3.1 and 3.2).

We shall consider the bound states near $y=0$ and use the condition $y_0 \gg a_B$, which allows us to set $x=y=0$ in Eq. (3.111) and this gives

$$u = -\frac{e^2}{(z^2+y_0^2)^{1/2}} \approx -\frac{e^2}{y_0} + \frac{e^2}{y_0^3} z^2. \tag{3.112}$$

Consequently, the Schrödinger equation for the motion along the z-axis becomes

$$\frac{d^2 f}{dz^2} + \frac{2\mu}{\hbar^2}[E - E_0 - u(z)] f = 0, \tag{3.113}$$

where

$$E_0 = \frac{e\hbar B}{2\mu c} - \frac{Mc^2 F^2}{2B^2} \tag{3.114}$$

is the energy corresponding to the limit of the continuous spectrum.

In the case of the lower energy levels in a well the effective values of z_{eff} are small compared with y_0, so that we can use the expansion of Eq. (3.112) which obviously leads to an oscillator potential. The energy spectrum which is then determined is of the form[76]

$$\frac{E_n - E_0}{2\text{Ry}} = -\lambda^{-1} + \lambda^{-3/2}\left(n + \frac{1}{2}\right), \quad \lambda = \frac{M}{\mu}\,\frac{\hbar c}{e^2}\,\frac{F}{B}\,\frac{B}{B_0}. \tag{3.115}$$

In the case of the hydrogen atom subjected to a field $B \sim B_0$ and also to fields F compatible with Eq. (3.110) the binding energy is of the order of 0.55 eV when the separation between the levels is ~ 0.1 eV.

4. CONCLUSIONS

The above review demonstrates the recent rapid growth of interest in the Stark and Zeeman effects. On the one hand, this is due to numerous possible practical applications of these effects and, on the other, it is due to problems of fundamental nature associated with the dynamics of systems with nonseparable variables.

In applications of the Stark and Zeeman effects it is usually essential to know not just one parameter, but all the characteristics of an atom in fields F and B, such as the splitting of levels, line intensities, probabilities of radiative and autoionization decay, etc. The range of field intensities F and B, and of the quantum number n of atoms is very wide. Very frequently the values of F and B are determined by the parameters of the ambient medium, such as the temperature T and density N of a plasma, which can also range within very wide limits. Therefore, it is very important to have analytic results for the parameters of an atom in fields F and B, particularly in a clear form that would be suitable for the use in practical applications.

Many of the problems discussed above have not been finally solved. This applies particularly to an atom in a magnetic field, when the inability to separate variables greatly complicates the situation. Investigations of the behavior of an electron in this case by the methods of classical mechanics and discovery of stochastic regions of motion leave open the problems of the nature of the quantum motion and its correspondence to the classical motion. One would hope that this review will draw attention to these problems.

[1)] The validity of the approximations represented by Eqs. (2.33) and (2.36)–(2.39) was established by Gulyaev[14,16] who compared directly these approximations with the results of numerical calculations based on the Gordon formulas. However, this leaves the problem of analytic justification of these approximations by the classical method.

[2)] The intensities I_{π_0} and I_{σ_1} of the series are numerically small and, therefore, they are not included in Fig. 4.

[3)] It should be noted that the transformation of a wave function on approach of the energy E to the energy E_0 was first analyzed by L. I. Mandel'shtam and M. A. Leontovich in 1928 (see Ref. 30).

[4)] A complete expansion of Eq. (2.77) subject to Eq. (2.78) naturally involves powers of the classical parameter Fn^4.

[5)] The strong repulsion of terms demonstrated in Fig. 6 is only apparent and it is due to inaccuracies of the numerical procedure used in the calculations (see Ref. 38).

[6)] The electron spin is ignored, because an allowance for this spin simply shifts the energy levels by a constant amount. It should be pointed out that the concept of a strong magnetic field is modified if an atom has many electrons.[39]

[7)] In the calculations we have to allow for the change in the parameter Λ, the value of which is -1 in the range $0 \leqslant \theta \leqslant \pi/4$ and $+4$ in the range $\pi/2 \leqslant \theta \leqslant \pi$.

[8)] In order to simplify the subsequent notation, we altered (compared with Ref. 54) the symbols used for dimensional ($\hat{\rho}, \hat{p}, \ldots$) and dimensionless ($\rho, p$) variables.

[9)] We shall ignore the range of very strong fields $B/B_0 > 10^3$, where the problems of separation of variables of the center of inertia and of relative motion become important.[59]

[1] H. A. Bethe and E. E. Salpeter, *Quantum Mechanics in One- and Two-Electron Systems*, Springer Verlag, Berlin (1958) reprinted from: Handbuch der Physik (ed. by S. Flugge), Vol. 85, Springer Verlag, Berlin (1957), pp. 88–346 [Russ. transl., Fizmatgiz, M., 1960].
[2] L. D. Landau and E. M. Lifshitz *Quantum Mechanics: Non-Relativistic Theory*, 3rd ed., Pergamon Press, Oxford (1977) [Russ. original, Nauka, M., 1974].
[3] I. I. Sobelman, *Introduction to the Theory of Atomic Spectra*, Pergamon Press, Oxford (1973) [Russ. original later ed., Nauka, M., 1977].
[4] B. M. Smirnov, Usp. Fiz. Nauk **131**, 577 (1980) [Sov. Phys. Usp. **23**, 450 (1980)].
[5] V. S. Letokhov, V. I. Mishin, and A. A. Puretskiĭ, Khim. Plazmy No. 4, 224 (1977).
[6] R. J. Elliott and R. Loudon, J. Phys. Chem. Solids **15**, 196 (1960).
[7] H. Hasegawa and R. E. Howard, J. Phys. Chem. Solids **21**, 179 (1961).
[8] B. B. Kadomtsev, Zh. Eksp. Teor. Fiz. **58**, 1765 (1970) [Sov. Phys. JETP **31**, 945 (1970)].
[9] B. B. Kadomtsev and V. S. Kudryavtsev, Zh. Eksp. Teor. Fiz. **62**, 144 (1972) [Sov. Phys. JETP **35**, 76 (1972)].
[10] R. H. Garstang, Rep. Prog. Phys. **40**, 105 (1977).
[11] H. R. Griem, *Spectral Line Broadening by Plasmas*, Academic Press, New York (1974) [Russ. trans., Mir, M., 1978].
[12] V. S. Lisitsa, Usp. Fiz. Nauk **122**, 449 (1977) [Sov. Phys. Usp. **20**, 603 (1977)].
[13] K. J. Gordon, C. P. Gordon, and F. J. Lockman, Astrophys. J. **192**, 337 (1974).
[14] S. A. Gulyaev, Astron. Zh. **53**, 1010 (1976) [Sov. Astron. **20**, 573 (1976)].
[15] M. J. Seaton, Rep. Prog. Phys. **46**, 167 (1983).
[16] N. B. Delone and V. P. Kraĭnov, *Atom in a Strong Optical Field* [in Russian], Energoatomizdat, Moscow (1984).
[17] R. F. Stebbings and F. B. Dunning (eds.), *Rydberg States of Atoms and Molecules*, Cambridge University Press (1983).
[18] G. F. Drukarev, Zh. Eksp. Teor. Fiz. **75**, 473 (1978) [Sov. Phys. JETP **48**, 237 (1978)]; **82**, 1388 (1982) [**55**, 806 (1982)].
[19] L. A. Bureeva, Astron. Zh. **45**, 1215 (1968) [Sov. Astron. **12**, 962 (1969)].
[20] S. P. Goreslavskiĭ, N. B. Delone, and V. P. Kraĭnov, Zh. Eksp. Teor. Fiz. **82**, 1789 (1982) [Sov. Phys. JETP **55**, 1032 (1982)].
[21] L. D. Landau and E. M. Lifshitz, *The Classical Theory of Fields*, 2nd ed., Pergamon Press, Oxford, 1962 [Russ. original, Fimatgiz, M., 1960].
[22] V. I. Kogan and A. B. Kukushkin, Zh. Eksp. Teor. Fiz. **87**, 1164 (1984) [Sov. Phys. JETP **60**, 665 (1984)].
[23] A. B. Kukushkin and V. S. Lisitsa, Zh. Eksp. Teor. Fiz. **88**, 1570 (1985) [Sov. Phys. JETP **61**, 937 (1985)].
[24] D. R. Herrick, Phys. Rev. A **26**, 323 (1982).
[25] J. R. Hiskes, C. B. Tarter, and D. A. Moody, Phys. Rev. **133**, A424 (1964).
[26] S. A. Gulyaev, Astron. Zh. **55**, 1002 (1978) [Sov. Astron. **22**, 572 (1978)].

[27]B. M. Smirnov and M. I. Chibisov, Zh. Eksp. Teor. Fiz. **49**, 841 (1965) [Sov. Phys. JETP **22**, 585 (1966)].
[28]R. Ya. (J.) Damburg and V. V. Kolosov, J. Phys. B **11**, 1921 (1978).
[29]R. Ya. Damburg and V. V. Kolosov, *Asymptotic Approach to the Stark Problem in the Case of the Hydrogen Atom* [in Russian], Zinatne, Riga (1977).
[30]B. B. Kadomtsev, V. I. Kogan, B. M. Smirnov, and V. D. Shafranov, Usp. Fiz. Nauk **124**, 547 (1978) [Sov. Phys. Usp. **21**, 272 (1978)].
[31]D. Banks and J. G. Leopold, J. Phys. B **11**, 37 (1978).
[32]D. F. Zaretskiĭ and V. P. Kraĭnov, Zh. Eksp. Teor. Fiz. **67**, 1301 (1974) [Sov. Phys. JETP **40**, 647 (1975)].
[33]M. B. Kadomtsev and B. M. Smirnov, Zh. Eksp. Teor. Fiz. **80**, 1715 (1981) [Sov. Phys. JETP **53**, 885 (1981)].
[34]C. Lanczos, Z. Phys. **62**, 518 (1930).
[35]N. Froman and P. O. Froman, *JWKB Approximation*, North-Holland, Amsterdam, 1965 [Russ. transl. Mir, M., 1967].
[36]D. S. Bailey, J. R. Hiskes, and A. C. Riviere, Nucl. Fusion **5**, 41 (1965).
[37]N. Hoe, B. D'Etat, and G. Coulaud, Phys. Lett. A **85**, 327 (1981).
[38]M. L. Zimmerman, M. G. Littman, M. M. Kash, and D. Klepner, Phys. Rev. A **20**, 2251 (1979).
[39]A. R. P. Rau, R. O. Mueller, and L. Spruch, Phys. Rev. A **11**, 1865 (1975).
[40]A. Galindo and P. Pascual, Nuovo Cimento B **34**, 155 (1976).
[41]H. C. Praddaude, Phys. Rev. A **6**, 1321 (1972).
[42]J. Simola and J. Virtamo, J. Phys. B **11**, 3309 (1978).
[43]D. Cabib, E. Fabri, and G. Fiorio, Nuovo Cimento B **10**, 185 (1972).
[44]A. G. Zhilich and B. S. Monozon, Fiz. Tverd. Tela (Leningrad) **8**, 3559 (1966) [Sov. Phys. Solid State **8**, 2846 (1967)].
[45]M. L. Zimmerman, M. M. Kash, and D. Kleppner, Phys. Rev. Lett. **45**, 1092 (1980).
[46]C. W. Clark and K. T. Taylor, J. Phys. B **13**, L737 (1980).
[47]E. A. Solov'ev, Zh. Eksp. Teor. Fiz. **82**, 1762 (1982) [Sov. Phys. JETP **55**, 1017 (1982)].
[48]D. R. Herrick, Phys. Rev. **26**, 323 (1982).
[49]M. Robnik, J. Phys. A **14**, 3195 (1981).
[50]A. I. Baz', Ya. B. Zel'dovich, and A. M. Perelomov, *Scattering, Reactions, and Decay in Nonrelativistic Quantum Mechanics, Israel program for Scientific Translations*, Jerusalem; Wiley, New York (1969) [Russ. original, Nauka, M., 1971 (2nd ed.)].
[51]P. A. Braun, Zh. Eksp. Teor. Fiz. **84**, 850 (1983) [Sov. Phys. JETP **57**, 492 (1983)].
[52]A. P. Kazantsev, V. L. Pokrovskii (Pokrovsky), and J. Bergou, Phys. Rev. A **28**, 3659 (1983).
[53]H. Forster, W. Strupat, W. Rosner, G. Wunner, H. Ruder, and H. Herold, J. Phys. B **17**, 1301 (1984).
[54]J. B. Delos, S. K. Knudson, and D. W. Noid, Phys. Rev. A **30**, 1208 (1984).
[55]A. H. Lichtenberg and M. A. Liberman, *Regular and Stochastic Motion*, Springer Verlag, Berlin 1983 [Russ. transl., Mir., M., 1984].
[56]G. Wunner, H. Ruder, and H. Herold, Phys. Lett. A **85**, 430 (1981).
[57]V. B. Pavlov-Verevkin and B. I. Zhilinskiĭ, Phys. Lett. A **75**, 279 (1980).
[58]H. Friedrich, Phys. Rev. A **26**, 1827 (1982).
[59]H. Herold, H. Ruder, and G. Wunner, J. Phys. B **14**, 751 (1981).
[60]G. Wunner, H. Ruder, and H. Herold, Phys. Lett. A **85**, 430 (1981).
[61]W. Rosner, G. Wunner, H. Herold, and H. Ruder, J. Phys. B **17**, 29 (1984).
[62]N. Hoe, H. W. Drawin, and L. Herman, J. Quant. Spectrosc. Radiat. Transfer. **7**, 429 (1967).
[63]A. V. Demura, V. S. Lisitsa, Zh. Eksp. Teor. Fiz. **62**, 2161 (1972) [Sov. Phys. JETP **35**, 1130 (1972)].
[64]L. P. Gor'kov and I. E. Dzyaloshinskii, Zh. Eksp. Teor. Fiz. **53**, 717 (1967) [Sov. Phys. JETP **26**, 449 (1968)].
[65]C. P. Slichter, *Principles of Magnetic Resonance with Examples from Solid State Physics*, Harper and Row, N. Y., 1963 [Russ. transl., Mir., M., 1968].
[66]T. Ishimura, J. Phys. Soc. Jpn. **23**, 422 (1967).
[67]V. S. Lisitsa, Opt. Spektrosk. **31**, 862 (1971) [Opt. Spectrosc. (USSR) **31**, 468 (1971)].
[68]N. L. Manakov and L. P. Rapoport, Zh. Eksp. Teor. Fiz. **69**, 842 (1975) [Sov. Phys. JETP **42**, 430 (1975)].
[69]V. S. Lisitsa and G. V. Sholin, Zh. Eksp. Teor. Fiz. **61**, 912 (1971) [Sov. Phys. JETP **34**, 484 (1972)].
[70]Yu. N. Demkov, V. N. Ostrovskiĭ, and E. A. Solov'ev, Zh. Eksp. Teor. Fiz. **66**, 125 (1974) [Sov. Phys. JETP **39**, 57 (1974)].
[71]M. Born, The Mechanics of the Atom, G. Bell and Sons, London, 1927 [Russ. transl., ONTI. M., 1934].
[72]G. L. Kotkin and V. G. Serbo, *Collection of Problems on Classical Mechanics* [in Russian], Nauka, Moscow (1977).
[73]Yu. N. Demkov, B. S. Monozon, and V. N. Ostrovskiĭ, Zh. Eksp. Teor. Fiz. **57**, 1431 (1969) [Sov. Phys. JETP **30**, 775 (1970)].
[74]E. A. Solov'ev, Zh. Eksp. Teor. Fiz. **85**, 109 (1983) [Sov. Phys. JETP **58**, 63 (1983)].
[75]A. V. Turbiner, Zh. Eksp. Teor. Fiz. **84**, 1329 (1983) [Sov. Phys. JETP **57**, 770 (1983)].
[76]L. A. Burkova, I. E. Dzyaloshinskiĭ, G. F. Drukarev, and B. S. Monozon, Zh. Eksp. Teor. Fiz. **71**, 526 (1976) [Sov. Phys. JETP **44**, 276 (1976)].

Translated by A. Tybulewicz